

The 2011 off the Pacific coast of Tohoku earthquake and response of high-rise buildings under long-period ground motions

I. Takewaki^{*}, S. Murakami, K. Fujita, S. Yoshitomi and M. Tsuji

*Department of Architecture and Architectural Engineering, Kyoto University
Kyotodaigaku-Katsura, Nishikyo-ku, Kyoto 615-8540, Japan*

ABSTRACT

In the afternoon of March 11, 2011, the eastern Japan was severely attacked by the 2011 off the Pacific coast of Tohoku earthquake (the Great East Japan earthquake). Nearly 30,000 people were killed or are still missing by that earthquake and the ensuing monster tsunami as of April 11, 2011. This paper reports some aspects of this devastating earthquake which hit an advanced country in seismic resistant design. It has been reported that long-period ground motions were induced in Tokyo, Nagoya and Osaka. The properties of these long-period ground motions are discussed from the viewpoint of critical excitation and the seismic behavior of two steel buildings of 40 and 60 stories subjected to the long-period ground motion recorded at Shinjuku, Tokyo is determined and discussed. This paper also reports the effectiveness of visco-elastic dampers like high-hardness rubber dampers in the reduction of responses of super high-rise buildings subjected to such long-period ground motions. The response reduction rate is investigated in detail in addition to the maximum response reduction. In December 2010 before this earthquake, simulated long-period ground motions for earthquake resistant design of high-rise buildings were provided in three large cities in Japan (Tokyo, Nagoya and Osaka) and nine areas were classified. Two 40-story steel buildings (slightly flexible and stiff) are subjected to these long-period ground motions in those nine areas for the detailed investigation of response characteristics of super high-rise buildings in various areas.

Key words: earthquake, disaster, long-period ground motion, high-rise building, critical excitation, input energy

^{*}Corresponding author, E-mail: takewaki@archi.kyoto-u.ac.jp
This paper is an improved version of the preliminary report [1].

1. Introduction

The most devastating earthquake in Japan after the 1923 Great Kanto earthquake hit the eastern Japan in the afternoon of March 11, 2011 [2]. The moment magnitude 9.0 earthquake is one of the five most powerful earthquakes in the world since modern record-keeping began in 1900. It was made clear afterwards that the recording system for low-frequency and large-amplitude ground motions was not sufficient in Japan and the first preliminary Japan Meteorological Agency (JMA) magnitude was smaller than 8 (7.9 exactly). The JMA magnitude was revised immediately as 8.4. The records of earthquake ground motions outside Japan were then used to determine the exact moment magnitude of 9.0 (intermediate announcement was 8.8). The earthquake resulted from the thrust faulting near the subduction zone plate boundary between the Pacific and North America Plates [2-4].

Nearly 30,000 people were killed or are still missing by this great earthquake and the ensuing monster tsunami as of April 11, 2011. The maximum height of the tsunami was reported to have attained almost 40m (Miyako City, Iwate Prefecture) and this was observed in the bay area with complex shapes. It was also reported that the tsunami arrived at the third or fourth story in some buildings and invaded over 5km from the coast line (Natori City, Miyagi Prefecture). It should be remarked that the number of collapsed (or damaged) buildings and houses remains not clear because most of the damages resulted from the tsunami and a clear record was not left. More detailed data on this earthquake can be obtained from the National Research Institute for Earth Science and Disaster Prevention (NIED) of Japan.

Because super high-rise buildings in mega cities in Japan have never been shaken by the so called long-period ground motions with high intensities, the response of high-rise buildings to such long-period ground motions is now one of the most controversial subjects in the field of earthquake-resistant design in Japan [5]. The issue of long-period ground motion and its effect on building structural design was initially brought up in Mexico, USA and Japan during 1980-1990s (for example [6-8]). Some clear observations have actually been reported recently

(most famous one is the severe sloshing in oil tanks during the Tokachioki earthquake, Japan in 2003 [9]) and the earthquake ground motions in Tokyo and Osaka during the March 11, 2011 earthquake are regarded to be extremely influential for super high-rise buildings. In December, 2010 just before this earthquake, a set of simulated long-period ground motions was provided by the Japanese Government [5] for the retrofit of existing high-rise buildings and as a design guideline for new high-rise buildings.

This paper describes first the characteristics of this 2011 earthquake and discusses the properties of long-period ground motions from the viewpoint of critical excitation, i.e. the phenomenon of resonance characterized by the coincidence of the predominant period of ground motions with the fundamental natural period of high-rise buildings. It is shown that the criticality of the long-period ground motions can be investigated based on the theory of critical excitation [10-13]. This theory is intended to overcome the difficulty resulting from the uncertainty of earthquake ground motions (for example [14]). The credible bounds of input energy responses are obtained by using the critical excitation method with the constraints on acceleration and velocity powers. It is demonstrated that the long-period ground motions can be controlled primarily by the velocity power and the ground motion recorded in Tokyo during the 2011 off the Pacific coast of Tohoku earthquake actually included fairly large long-period wave components.

Furthermore, assumed 40 and 60-story steel buildings are subjected to such long-period ground motion as recorded in Shinjuku, Tokyo during the 2011 off the Pacific coast of Tohoku earthquake. It is shown that high-hardness rubber dampers, a kind of visco-elastic dampers, are able to damp the building vibration during long-period ground motions in an extremely shorter duration than in case of the building without those dampers. Two assumed 40-story steel buildings are also subjected to a set of simulated long-period ground motions taken from a December 2010 document of the Japanese Government [5] for the detailed investigation of response characteristics of super high-rise buildings under many simulated long-period ground

motions in various areas.

2. General characteristics of the 2011 off the Pacific coast of Tohoku earthquake

The general characteristics of the 2011 off the Pacific coast of Tohoku earthquake are described first. The source inversion and slip distribution using near-source strong ground motions are shown in Fig.1 [15]. Since it is necessary to understand the size of the 2011 earthquake, the comparison of slipped fault size is shown in Fig.2 among the 2004 Sumatra earthquake (M=9.1), the 1923 Great Kanto earthquake (M=7.9), the 1995 Hyogoken-Nanbu (Kobe) earthquake (M=7.3) and the 2011 off the Pacific coast of Tohoku earthquake (M=9.0) [16]. Due to the large magnitude and the distance from the source to the Honshu island of Japan, fairly wide areas in the eastern Japan were influenced and shaken by this earthquake.

The representative near-source ground motions along the Pacific coast in the eastern Japan are illustrated from north to south in Fig.3(a) [17]. It can be found out that two or more series (or groups) of waves exist in some areas and most ground motions continue for over 2 minutes. This implies the repeated occurrence of the fault slips in wide areas. This phenomenon has been pointed out by many researchers (for example [18-20]). It was reported afterwards that three main fault slips occurred in this series of events, i.e. the first at the eastern side of Sendai City (off Miyagi Prefecture), the second at the southern (off Miyagi and Fukushima Prefectures) and northern (off Iwate Prefecture) parts of the first one and the third at the further southern side of the second slip (off Ibaragi Prefecture).

Fig.3(b) presents a more detailed description of those recorded ground motions (Yellow star indicates the epicenter). The following is the interpretation by NIED of Japan [21]. In Tohoku area (from Iwate Prefecture through Fukushima Prefecture), two wave groups (pink and yellow colors) can be observed from the vicinity of the epicenter (star mark). This means that main fault ruptures occurred twice in the vicinity of the epicenter one after another. In Fukushima Prefecture, a wave group (blue color) can be observed around 200(s) towards the

north. There are intensive waves between the yellow arrow and the blue arrow. In Ibaragi Prefecture, a wave group (blue color arrow downward) can be seen. These results imply that a fault rupture occurred around the epicenter and this rupture induced many subsequent ruptures.

It is believed that the data of ground motions in Fig.3 are very useful for the investigation of the accuracy of methods for constructing the ground motions from several sources. The distributions of the maximum ground accelerations and the maximum ground velocities determined from K-NET and KiK-net (NIED) data are shown in Fig.4 [22].

Table 1 shows the top ten largest observed peak ground accelerations during this earthquake [17]. It is found that the maximum ground acceleration over 2.9g was recorded at the K-NET station of Tsukidate in Kurihara City of Miyagi Prefecture. However it is reported that the predominant period of this ground motion is shorter than 0.3s and this ground motion did not affect most buildings so much. These ground motion characteristics are common in almost all the areas along the Pacific coast in the eastern Japan and the damage to buildings is not so large in spite of the tremendous magnitude of 9.0. The damages of most buildings are thought to result from the monster tsunami.

Other peculiar points observed in this 2011 earthquake may be a wide spread of liquefaction and settlement of land along the Pacific coast in Miyagi and Iwate Prefectures. It was reported that remarkable liquefaction occurred in many places on soft grounds including sands (over 42km² even in Tokyo bay area) and the settlement over 1m of land in Miyagi and Iwate Prefectures may result from the movement of plates near the epicenter. It is understood that the unexpected wide spread of liquefaction in spite of not so high level of maximum ground acceleration results from the long duration of shaking (over 2 minutes and four times longer than Hyogoken-Nanbu earthquake). It is thought that this long duration of shaking caused a rapid increase of excess pore water pressure. The liquefaction was also observed in Tokyo bay area and it was reported that 14.5 km² experienced liquefaction in Urayasu City in Chiba prefecture (one of Tokyo bay area cities).

As stated above, one of the most important issues in mega cities like Tokyo, Osaka and Nagoya during this 2011 earthquake is the occurrence of long-period ground motions which could affect severely most super high-rise buildings through the resonant phenomenon. It is often reported that many super high-rise buildings in Tokyo and Osaka were severely shaken by those long-period ground motions. This issue will be discussed in the following sections in detail.

3. Seismic response simulation of super high-rise buildings in Tokyo

3.1 Properties of ground motions in Tokyo

Fig.5(a) shows the acceleration waveforms of the long-period ground motion recorded at K-NET, Shinjuku station (TKY007) [17] and Fig.5(b) presents the corresponding velocity waveforms [17]. It can be observed that the maximum ground velocity attains about 0.25(m/s) and the ground shaking continues for over several minutes. The velocity response spectra for 1 and 5% damping are shown in Fig.6 [17]. The corresponding ones of Japanese seismic design code for 5% damping are also plotted in Fig.6. It is understood that these ground motions include long-period components up to 10 seconds.

For investigating further the long-period characteristics of that record, the Fourier amplitude spectra of both acceleration and velocity records have been obtained. Fig.7 shows the Fourier amplitude spectra of accelerations of Fig.5(a) and Fig.8 illustrates those of velocities of Fig.5(b) [1].

3.2 Measure of criticality in long-period ground motions

Fig.9 explains the schematic diagram for computing credible bounds of the input energy per unit mass E_I/m to a single-degree-of-freedom (SDOF) model for acceleration and velocity constraints [11-13]. The function $F(\omega)$ in the diagram indicates the energy transfer function defined by

$$F(\omega) = \frac{2h\Omega\omega^2}{\pi\{(\Omega^2 - \omega^2)^2 + (2h\Omega\omega)^2\}} \quad (1)$$

where Ω : natural circular frequency of the SDOF model, h : damping ratio and ω : the excitation frequency. The input energy per unit mass E_I/m to the SDOF model can then be expressed by

$$E_I/m = \int_0^\infty |A(\omega)|^2 F(\omega) d\omega \quad (2a)$$

or

$$E_I/m = \int_0^\infty |V(\omega)|^2 \omega^2 F(\omega) d\omega \quad (2b)$$

where $A(\omega)$ and $V(\omega)$ are the Fourier transforms of the ground motion acceleration and ground motion velocity, respectively. It can be observed from Fig.9 that the region of short natural period can be controlled by the credible bound for the acceleration constraint and the region of long period can be controlled by the credible bound for the velocity constraint. It may be concluded that the introduction of both credible bounds enables the construction of the credible bound with uniform risk in all the natural period range. The word of ‘uniform risk’ is used in the meaning that the ratio of the actual input energy to the corresponding credible bound is almost constant in some ground motions regardless of the natural period of the model.

Fig.10(a) presents the comparison of the actual input energies (5% damping), the credible bounds [11-13] for acceleration constraints (acceleration power [23]) and the credible bounds for velocity constraints (velocity power [23]) for NS and EW components [1]. The intersection point implies the predominant period from the viewpoint of input energy. The periods of 4 and 6 seconds are such predominant periods of ground motions and this implies that the ground motion recorded at K-NET, Shinjuku station (TKY007) actually included fairly large long-period wave components. For comparison, Fig.10(b) shows the corresponding figures for El Centro NS 1940 and JMA Kobe NS 1995 (Hyogoken-Nanbu earthquake) [1, 11, 12]. The intersection point corresponds to rather shorter period ranges.

It may be concluded that the credible bound for the velocity constraint can control the bound of input energy from the long-period ground motion and this bound plays a role for overcoming the difficulties caused by uncertainties of long-period ground motions (predominant period and intensity level).

3.3 Seismic response simulation of super high-rise buildings in Tokyo

The 2011 off the Pacific coast of Tohoku earthquake may be the first earthquake to have occurred between tectonic plates and have affected super high-rise buildings in mega cities. In order to investigate the influence of the recorded long-period ground motions on high-rise buildings, two steel moment-resisting building frames of 40 and 60 stories have been studied in [1]. The 40-story building has a fundamental natural period of $T_1=4.14\text{s}$ and the 60-story building has a corresponding one of $T_1=5.92\text{s}$.

The buildings have a plan of $40\text{m}\times 40\text{m}$ (equally spaced 36 columns; span length=8m) and one planar frame is taken as the object frame. The uniform story height is 4m. The floor mass per unit area is assumed to be $800\text{kg}/\text{m}^2$. The damping ratio is taken as 0.01 in accordance with the well-accepted database [24]. The variability of damping ratio is large depending on amplitude, building usage, etc. and most of the data exist in 0.5-3.0% in high-rise steel buildings [24]. Therefore 1% damping (most credible one) has been used here. The cross-sectional properties of the 40-story steel building frame are shown in Table 2. The composite beam action (stiffening by floor slabs) has been taken into account. The stiffness of beams has been set as 1.5 times the original stiffness. The yield stress of the steel members is $235(\text{N}/\text{mm}^2)$. The rigid part of members is introduced at each beam-column connection.

It is well accepted that the passive dampers are very effective in the reduction of earthquake response in high-rise buildings. For the purpose of clarifying the merit of visco-elastic dampers (high-hardness rubber dampers [25] (see Fig.11)), the buildings of 40 and 60 stories without and with these high-hardness rubber dampers have been subjected to the

long-period ground motion recorded at K-NET, Shinjuku station (TKY007). The outline of the high-hardness rubber dampers is shown in Fig.11. One damper unit consists of rubber thickness=15mm and rubber area=0.96m². The frame includes 4 damper units at every story.

Fig.12 shows the maximum story displacements and interstory drifts of the 40-story building of $T_1=4.14s$ without or with high-hardness rubber dampers to ground motion at Shinjuku station (TKY007) (frame response: elastic or elastic-plastic) [1]. It can be understood that linear and non-linear analyses provide nearly the same results in this case. On the other hand, Fig.13 illustrates the maximum story displacements and interstory drifts of the 60-story building of $T_1=5.92s$ without or with high-hardness rubber dampers to ground motion at Shinjuku station (TKY007) (frame response: elastic-plastic, '4 dampers per story' corresponds to 'damper double') [1]. Only non-linear analyses have been performed. It can be observed that high-hardness rubber dampers are effective for the reduction of displacements.

Table 3 shows the comparison of the maximum absolute accelerations at the top between the 60-story buildings without and with high-hardness rubber dampers under three recorded ground motions (EW component of TKY007, EW component at Chiyoda-ku station near Shinjuku station and NS component at Osaka WTC) during the 2011 off the Pacific coast of Tohoku earthquake. It can be seen that the top acceleration is reduced by the introduction of the high-hardness rubber dampers.

Fig.14(a) presents the comparison of time histories of top-story displacements of the assumed 60-story building of $T_1=5.92s$ to ground motion at Shinjuku station (EW component of TKY007) during the 2011 off the Pacific coast of Tohoku earthquake (frame response: elastic-plastic, without or with high-hardness rubber dampers) [1]. It can be understood that the high-hardness rubber dampers can damp the building vibration in an extremely short duration. It should be remarked that this ground motion was recorded for 300s and the response after 300s is a free vibration in this case. Fig.14(b) shows a similar comparison to ground motion (EW component) at Chiyoda-ku station near Shinjuku station during the 2011 off

the Pacific coast of Tohoku earthquake. It can be understood that the longer ground motion duration of 600(s) can demonstrate well the damping performance of the high-hardness rubber dampers.

It has been reported recently [26] that a 54-story building (height=223m: fundamental natural period=6.2s (short-span direction), 5.2s (long-span direction)) retrofitted with passive oil dampers including the supporting bracing system in Shinjuku, Tokyo experienced a top displacement of 0.54(m) during the 2011 off the Pacific coast of Tohoku earthquake. The vibration duration has been reported to be over 13 minutes. It has also been found that the building would have attained a top displacement of 0.7(m) if the passive dampers had not been installed. This fact corresponds well to the result explained above.

There is another report that a 55-story super high-rise building in Osaka (height=256m: fundamental natural period=5.8s (long-span direction), 5.3s (short-span direction)) was shaken severely regardless of the fact that Osaka is located far from the epicenter (about 800km) and the JMA instrumental intensity was 3 in Osaka. It should be pointed out that the level of velocity response spectra of ground motions observed here (first floor) is almost the same as that at the Shinjuku station (K-NET) in Tokyo and the top-story displacement are about 1.4m (short-span direction) and 0.9m (long-span direction). This implies the need of consideration of long-period ground motions in the seismic resistant design of super high-rise buildings in mega cities even though the site is far from the epicenter.

4. Seismic response of high-rise buildings to simulated long-period ground motions (Japanese Government action)

4.1 Characteristics of simulated long-period ground motions

On December 21, 2010, the Japanese Government made a press release to upgrade the regulation for high-rise buildings under long-period ground motions. The Ministry of Land, Infrastructure, Transport and Tourism (MLIT) of Japan specified 9 areas in Tokyo, Nagoya and

Osaka (see Fig.15) [5]. Areas 1-4 exist in Tokyo, areas 5-7 in Nagoya and areas 8, 9 in Osaka.

Fig.16 shows the acceleration and velocity records of simulated ground motions in those 9 areas specified in Fig.15. These simulated ground motions were generated by using the acceleration response spectra (5%) at the bedrock and the group delay time (mean and standard deviation) for the phase property [5]. It can be observed that large velocity waves appear in later times.

Fig.17 presents the pseudo velocity response spectra and velocity response spectra of the simulated acceleration ground motions specified by the MLIT. It can be seen that the velocity spectra in 2-8 seconds have relatively large magnitudes.

Fig.18 shows the actual input energies per unit mass [11, 12, 22], the credible bounds for acceleration constraints [11, 12] and the credible bounds for velocity constraints [11, 12] for the simulated ground motions specified by the MLIT. As stated before, the intersection point indicates the predominant period of the ground motion. As in the ground motion recorded at K-NET, Shinjuku station (TKY007), 3-8 seconds are such predominant periods and this implies that the simulated ground motions actually include fairly large long-period wave components.

4.2 Response simulation of super high-rise buildings without and with high-hardness rubber dampers

In order to investigate the influence of the simulated ground motions in areas 1-9 on the response of high-rise buildings, two buildings of 40 stories have been assumed. The parameters of the buildings are the same as those stated in Section 3.3. The stiffness of beams has been evaluated as double the original stiffness for the building frame of $T_1=3.6s$ and as 1.5 times the original stiffness for the building frame of $T_1=4.14s$. Judging from the database on the relationship of the building height with its fundamental natural period in Japan, the model of $T_1=3.6s$ is a slightly stiff building model for 40-story steel buildings and the model of $T_1=4.14s$ is a slightly flexible steel building model. Only the latter one has been treated in Section 3.

For the purpose of clarifying the merit of visco-elastic dampers (high-hardness rubber dampers [25] as in the previous case), the buildings of 40 stories without and with these high-hardness rubber dampers have been subjected to the simulated long-period ground motions. One damper unit consists of rubber thickness=15mm and rubber area=0.96m². ‘Damper single’ includes 2 damper units at every story and ‘damper double’ includes 4 damper units at every story.

Fig.19 illustrates the comparison of the time histories of the top displacement of the 40-story buildings of $T_1=3.6s$ without and with high-hardness rubber dampers (frame response; elastic) under a simulated long-period ground motion in area 5 (Nagoya area). It can be observed that the high-hardness rubber dampers are able to damp the building vibration during long-period ground motions in an extremely shorter duration compared to the building without those dampers.

Fig.20 presents the time histories of the top displacement of the 40-story buildings of $T_1=3.6s$ without and with high-hardness rubber dampers (frame response; elastic) under simulated long-period ground motions in nine areas. It can be found that the responses in area 5 and area 7 (Nagoya area) are large. Fig.21 shows the maximum interstory drifts of the 40-story buildings of $T_1=3.6s$ without and with high-hardness rubber dampers (frame response; elastic). It can also be understood that the maximum response of the damper double is not different much from that of the damper single and the damper single is sufficient for the maximum response reduction in this case. However as for the reduction rate of the vibration, the damper double is better than the damper single.

Fig.22 illustrates the time histories of the top displacement of the 40-story buildings of $T_1=4.14s$ without and with high-hardness rubber dampers (frame response; elastic). It can be seen that the responses are quite different from those of $T_1=3.6s$ shown in Fig.20. This characteristic may depend on the relation of the fundamental natural period of the building with the predominant period of ground motions in nine areas. Fig.23 shows the maximum interstory

drifts of the 40-story buildings of $T_1=4.14s$ without and with high-hardness rubber dampers (frame response; elastic). Different from the case for $T_1=3.6s$ shown in Fig.21, the maximum response of the damper double is much smaller than that of the damper single especially in area 7 which shows the maximum response. This indicates the superiority of the increase of damper quantity in the reduction of the maximum response in addition to the reduction rate of the vibration.

Fig.24 presents the comparison of the top displacements of the 40-story buildings of $T_1=3.6(s)$ (elastic or elastic-plastic, without or with dampers) under the simulated long-period ground motion in area 5. It can be observed that the elastic-plastic response of the building frame decreases the response level to some extent. However it can also be seen that the high-hardness rubber dampers can damp the vibration so quickly. It has been confirmed that this quick vibration reduction rate can be achieved also by viscous dampers like oil dampers so long as an appropriate amount of dampers is provided. Fig.25 shows the maximum interstory drifts of 40-story buildings of $T_1=3.6s$ (Area 5) and $T_1=4.14s$ (Area 7) without high-hardness rubber dampers (elastic or elastic-plastic). As in Fig.24, it can be seen that the elastic-plastic response of the building frame decreases the response level to some extent. Since the plastic deformation may cause some problems in the beam-column connections (as observed during Northridge and Hyogoken-Nanbu earthquakes) and member plastic deformation capacities, a more detailed investigation will be necessary on the overall characteristics of this property. Fig.26 illustrates the plastic-hinge formation diagram of the building frames without and with dampers. The non-linear analyses performed take into account both material and geometrical non-linearities.

The purposes of this paper (Section 4) are to disclose the general properties of the effect of simulated long-period ground motions on the responses of high-rise buildings and to investigate the effect of high-hardness rubber dampers in the vibration reduction of high-rise buildings under long-period ground motions. For these purposes only elastic responses have

been investigated comprehensively at first (Figs.20-23). This treatment is valid when high strength steels are used (this is often the case now in Japan), because the response will be almost within the elastic limit. However, since it seems to be also useful to investigate the effect of elastic-plastic behavior on the resonant phenomenon, the comparison between elastic and elastic-plastic responses have been conducted for the model of $T_1=3.6s$ in Area 5 and that of $T_1=4.14s$ in Area 7 as representative ones. As can be seen from Fig.20, most of the responses are within the elastic limit except in a few cases including Areas 5 and 7. Furthermore it was made clear that most responses of high-rise buildings in Japan (Tokyo and Osaka) during the 2011 off the Pacific coast of Tohoku earthquake are within the elastic limit. It seems reasonable to a limited extent also from these viewpoints to deal with the elastic response of high-rise buildings under simulated long-period ground motions.

4.3 AIJ's research result

Architectural Institute of Japan (AIJ) made a press release on March 4, 2011 just one week before the March 11, 2011 earthquake on the result of their research on the response of high-rise buildings under long-period ground motions [27]. The conclusions in this press release may be summarized as follows:

- (1) High-rise buildings in Tokyo, Nagoya and Osaka may experience long-duration vibration under simulated long-period ground motions obtained as a sequence of Tokai, Tonankai and Nankai earthquakes. However the collapse will not occur (the possibility may be very low).
- (2) The long-period ground motions exhibit different properties in different areas. The high-rise buildings also have different properties depending on their heights and constructed periods. The relation of the structural properties of high-rise buildings with the properties of long-period ground motions plays a key role in the evaluation of seismic response of high-rise buildings.

- (3) The damage to non-structural components, facilities and furniture may be caused easily. Such damage can be reduced effectively by introducing appropriate steps.
- (4) Passive dampers will be able to damp the building vibration remarkably and reduce the damage to structural members.

5. Conclusions

The following conclusions have been obtained.

- (1) The 2011 off the Pacific coast of Tohoku earthquake is the most devastating earthquake in Japan after the 1923 Great Kanto earthquake in terms of the damaged area and loss cost. This earthquake may be the largest inter-plate earthquake which attacked mega cities after the construction of super high-rise buildings. However it is reported that this earthquake may not be the most influential one because the influence depends on the plate (including epicenter) on which mega cities lie. This fact has been confirmed from the comparison with the result using the simulated ground motions provided by the Japanese Government in December 2010.
- (2) The ground motion recorded at K-NET, Shinjuku station (TKY007), Tokyo during the 2011 off the Pacific coast of Tohoku earthquake contains fairly large long-period wave components and has a frequency content of broad band (2-6 seconds). This can be observed from not only the velocity response spectra (and Fourier spectra) but also the earthquake input energy spectra taking into account of the concept of critical excitation. This characteristic has also been demonstrated through the simulated ground motions provided by the Japanese Government in December 2010.
- (3) The region of short natural period in the input energy spectrum can be controlled by the credible bound for the acceleration constraint and the region of long period can be controlled by the credible bound for the velocity constraint [11-13]. The introduction of both credible bounds enables the construction of the credible bound with uniform risk

(almost constant ratio of the input energy to its credible bound) in all the natural period range in some ground motions. The credible bound [11-13] for the velocity constraint can control the bound of input energy from the long-period ground motion and this bound plays a role for overcoming the difficulties caused by uncertainties of long-period ground motions.

- (4) Visco-elastic dampers like high-hardness rubber dampers and viscous dampers like oil dampers are able to damp the building vibration during long-period ground motions in an extremely shorter duration compared to the building without those dampers. It has been made clear from this March 11, 2011 earthquake that the safety is not the only target and the functionality together with the consideration of psychological aspects of residents has to be protected appropriately.
- (5) The word ‘unpredicted incident’ is often used in Japan after this great earthquake. It may be true that the return period of this class of earthquakes at the same place could be 500-1000 years and the use of this word may be acceptable to some extent from the viewpoint of the balance between the construction cost and the safety. However, the critical excitation method is expected to enhance the safety of building structures against undesirable incidents drawn from this irrational concept in the future.

Acknowledgements

Part of the present work is supported by the Grant-in-Aid for Scientific Research of Japan Society for the Promotion of Science (No.21360267) and the joint project with Sumitomo Rubber Industry Corp. These supports are greatly appreciated. The use of ground motion records at K-NET, Nikken Sekkei Co. in Tokyo and Building Research Institute of Japan is also highly appreciated.

This paper is the second version of the preliminary report [1]. Some data in Figs.7, 8, 10, 12-14 are from Reference [1]. The first author is grateful to the editors of J. Zhejiang University, Science A for permitting the reuse of the data.

References

- [1] Takewaki, I. Preliminary report of the 2011 off the Pacific coast of Tohoku earthquake, *J. Zhejiang University-SCIENCE A*, **12**(5), 327-334, 2011.
- [2] Architectural Institute of Japan. Preliminary reconnaissance report on the 2011 Off the Pacific coast of Tohoku earthquake, April 6, 2011 (in Japanese).
- [3] NIED (National Research Institute for Earth Science and Disaster Prevention). 2011 Off the Pacific Coast of Tohoku earthquake. (in Japanese) (Available from <http://www.hinet.bosai.go.jp/topics/off-tohoku110311/> [Accessed on May 3, 2011]).
- [4] USGS. Magnitude 9.0 - NEAR THE EAST COAST OF HONSHU, JAPAN. (Available from <http://earthquake.usgs.gov/earthquakes/eqinthenews/2011/usc0001xgp/#summary> [Accessed on May 3, 2011]).
- [5] Ministry of Land, Infrastructure, Transport and Tourism (MLIT). Code draft for the retrofit of existing high-rise buildings and design guideline for new high-rise buildings, December 21, 2010 (in Japanese) (Available from http://www.mlit.go.jp/report/press/house05_hh_000218.html [Accessed on January 11, 2011]).
- [6] Heaton, T., Hall, J., Wald, D. and Halling, M.. Response of high-rise and base-isolated buildings to a hypothetical M 7.0 blind thrust earthquake, *Science*, **267**, 206-211, 1995.
- [7] Kamae, K, Kawabe, H and Irikura, K. Strong ground motion prediction for huge subduction earthquakes using a characterized source model and several simulation techniques, *Proc. of the 13th WCEE*, Vancouver, 2004.
- [8] Ariga, T., Kanno, Y. and Takewaki, I. Resonant behavior of base-isolated high-rise buildings under long-period ground motions. *The Structural Design of Tall and Special Buildings*, **15**(3), 325-338, 2006.
- [9] Zama, S., Nishi, H., Yamada, M., and Hatayama, K. Damage of oil storage tanks caused by liquid sloshing in the 2003 Tokachi Oki earthquake and revision of design spectra in the long-period range, Proceedings of the 14th World Conference on Earthquake Engineering,

October 12-17, 2008, Beijing, China.

- [10] Drenick, R. F. Model-free design of aseismic structures. *J. Engrg. Mech. Div.*, ASCE, **96**(EM4), 483-493, 1970.
- [11] Takewaki, I. Bound of earthquake input energy. *J. Struct. Engrg.*, ASCE, **130**(9), 1289-1297, 2004.
- [12] Takewaki, I. *Critical Excitation Methods in Earthquake Engineering*, Elsevier, 2006.
- [13] Takewaki, I. Critical excitation methods for important structures, invited as a Semi- Plenary Speaker, EURODDYN 2008, July 7-9, 2008, Southampton, England.
- [14] Geller, R.J., Jackson, D.D., Kagan, Y.Y., and Mulargia, F. Earthquakes cannot be predicted. *Science*, **275**, 1616, 1997.
- [15] NIED (National Research Institute for Earth Science and Disaster Prevention). 2011 Off the Pacific Coast of Tohoku earthquake. Source inversion and slip distribution using near-source strong ground motions. (in Japanese) (revised version in April 12, 2011 by W.Suzuki, M.Aoi and H.Sekiguchi) (Available from http://www.kyoshin.bosai.go.jp/kyoshin/topics/TohokuTaiheiyo_20110311/inversion/ [Accessed on May 3, 2011]).
- [16] Asahi newspaper, April 10, 2011 (in Japanese).
- [17] NIED (National Research Institute for Earth Science and Disaster Prevention). 2011 Off the Pacific Coast of Tohoku earthquake, Strong Ground Motion, Emergency meeting of Headquarters for Earthquake Research Promotion, March 13, 2011. (Available from http://www.k-net.bosai.go.jp/k-net/topics/TohokuTaiheiyo_20110311/nied_kyoshin2e.pdf, [Accessed on April 20, 2011]).
- [18] Elnashai, A, Bommer, JJ, and Martinez-Pereira, A. Engineering implications of strong motion records from recent earthquakes. *In: Proceedings of 11th European conference on earthquake engineering*. CD-ROM. Paris; 1998.
- [19] Hatzigeorgiou GD, Beskos DE. Inelastic displacement ratios for SDOF structures subjected to repeated earthquakes. *Engineering Structures*, **31**(13), 2744–55, 2009.

- [20] Moustafa, A., and Takewaki, I. Response of nonlinear single-degree-of-freedom structures to random acceleration sequences, *Engineering Structures*, **33**, 1251-1258, 2011.
- [21] NIED (National Research Institute for Earth Science and Disaster Prevention). 2011 Off the Pacific Coast of Tohoku earthquake: Overview (in Japanese) (Available from <http://www.hinet.bosai.go.jp/topics/off-tohoku110311/> [Accessed on May 3, 2011]).
- [22] NIED (National Research Institute for Earth Science and Disaster Prevention). 2011 Off the Pacific Coast of Tohoku earthquake, Strong Ground Motion. (in Japanese) (Available from http://www.kyoshin.bosai.go.jp/kyoshin/topics/html20110311144626/main_20110311144626.html [Accessed on April 20, 2011]).
- [23] Housner, G.W. and P.C.Jennings. The capacity of extreme earthquake motions to damage structures. *Structural and geotechnical mechanics* edited by W.J. Hall, 102-116, Prentice-Hall Englewood Cliff, NJ, 1975.
- [24] Satake, N, Suda, K., Arakawa, T., Sasaki, A. and Tamura, Y. Damping evaluation using full-scale data of buildings in Japan, *J. of Structural Eng. ASCE*, 129(4), 470-477, 2003.
- [25] Tani, T., Yoshitomi, S., Tsuji, M. and Takewaki, I. High-performance control of wind-induced vibration of high-rise building via innovative high-hardness rubber damper, *The Structural Design of Tall and Special Buildings*, **18**(7), 705-728, 2009.
- [26] Asahi newspaper, evening edition of April 19, 2011 (in Japanese).
- [27] Architectural Institute of Japan (AIJ). Report at the open research meeting on design guide for super high-rise buildings under long-period ground motions, March 4, 2011 (in Japanese).

Captions of figures and tables

- Fig.1 Source inversion and slip distribution using near-source strong ground motions [15]
- Fig.2 Fault size of 2004 Sumatra earthquake ($M=9.1$), 1923 Great Kanto earthquake ($M=7.9$), 1995 Hyogoken-Nanbu (Kobe) earthquake ($M=7.3$) and 2011 off the Pacific coast of Tohoku earthquake ($M=9.0$) (data from [16])
- Fig.3(a) Characteristics of near-source ground motions along Pacific coast in eastern Japan [17]
- Fig.3(b) Relation among fault rupture, wave propagation and ground motion sequences (Yellow star indicates the epicenter) [21]
- Fig.4 Maximum ground accelerations and maximum ground velocities determined from K-NET and KiK-net data [22]
- Fig.5(a) Long-period acceleration ground motion recorded at K-NET, Shinjuku station (TKY007)
- Fig.5(b) Long-period velocity ground motion recorded at K-NET, Shinjuku station (TKY007)
- Fig.6 Velocity response spectra (5% and 1% damping) of ground motions at Shinjuku station (TKY007) and the corresponding ones of Japanese seismic design code for 5% damping
- Fig.7 Fourier amplitude spectra of acceleration ground motion at K-NET, Shinjuku station (TKY007)
- Fig.8 Fourier amplitude spectra of velocity ground motion at K-NET, Shinjuku station (TKY007)
- Fig.9 Schematic diagram for computing credible bounds for acceleration and velocity constraints
- Fig.10(a) Actual input energies per unit mass (5% damping), the credible bounds for acceleration constraints and the credible bounds for velocity constraints for the ground motions at K-NET, Shinjuku station (TKY007)
- Fig.10(b) Actual input energies per unit mass (5% damping), the credible bounds for acceleration constraints and the credible bounds for velocity constraints for El Centro NS (1940) and JMA Kobe NS (1995)
- Fig.11 High-hardness rubber dampers; (a) Overview, (b) Modeling into three elements
- Fig.12 (a) Maximum story displacement and (b) maximum interstory drift of a 40-story building of $T_1=4.14$ s without or with high-hardness rubber dampers to ground motion at Shinjuku station (TKY007) during the 2011 off the Pacific coast of Tohoku earthquake (frame response: elastic or elastic-plastic)
- Fig.13 (a) Maximum story displacement and (b) maximum interstory drift of a 60-story building of $T_1=5.92$ s without or with high-hardness rubber dampers to ground motion at Shinjuku station (TKY007) during the 2011 off the Pacific coast of Tohoku earthquake (frame response: elastic-plastic, '4 dampers per story' corresponds to 'damper double')
- Fig.14(a) Comparison of time histories of top-story displacement of an assumed 60-story building of $T_1=5.92$ s without or with high-hardness rubber dampers to ground motion at Shinjuku station (EW component of TKY007) during the 2011 off the Pacific coast of

Tohoku earthquake (frame response: elastic-plastic)

Fig.14(b) Comparison of time histories of top-story displacement of an assumed 60-story building of $T_1=5.92s$ without or with high-hardness rubber dampers to ground motion (EW component) at Chiyoda-ku station near Shinjuku station during the 2011 off the Pacific coast of Tohoku earthquake (frame response: elastic-plastic)

Fig.15 Nine areas in Osaka, Nagoya and Tokyo specified by the MLIT of Japan [5]

Fig.16 Acceleration and velocity ground motion records at 9 areas specified by the MLIT of Japan (data from [5])

Fig.17 Pseudo velocity response spectra (5% damping) and velocity response spectra of the simulated acceleration ground motions specified by the MLIT of Japan [5]

Fig.18 Actual input energies per unit mass (5% damping), the credible bounds for acceleration constraints and the credible bounds for velocity constraints for the simulated ground motions specified by the MLIT of Japan

Fig.19 Comparison of the time histories of the top displacement of the 40-story buildings of $T_1=3.6s$ without and with high-hardness rubber dampers (frame response; elastic) under a simulated long-period ground motion in area 5

Fig.20 Time histories of top displacement of 40-story buildings of $T_1=3.6s$ without and with high-hardness rubber dampers (frame response; elastic)

Fig.21 Maximum interstory drifts of 40-story buildings of $T_1=3.6s$ without and with high-hardness rubber dampers (frame response; elastic)

Fig.22 Time histories of top displacement of 40-story buildings of $T_1=4.14s$ without and with high-hardness rubber dampers (frame response; elastic)

Fig.23 Maximum interstory drifts of 40-story buildings of $T_1=4.14s$ without and with high-hardness rubber dampers (frame response; elastic)

Fig.24 Top displacement of 40-story buildings of $T_1=3.6(s)$ without and with high-hardness rubber dampers (frame response: elastic or elastic-plastic) (Area 5)

Fig.25 Maximum interstory drifts of 40-story buildings of $T_1=3.6s$ and $T_1=4.14s$ without high-hardness rubber dampers (frame response; elastic or elastic-plastic), (a) 40-story building of $T_1=3.6s$ in Area 5, (b) 40-story building of $T_1=4.14s$ in Area 7

Fig.26 Plastic-hinge formation in 40-story buildings of $T_1=3.6(s)$ without and with high-hardness rubber dampers (Area 5)

Table 1 List of 10 largest observed peak ground accelerations [17]

Table 2 Cross sections of members

Table 3 Reduction of top acceleration via high-hardness rubber dampers (m/s^2)

Table 1 List of 10 largest observed peak ground accelerations [17]

	Station name	PGA	JMA instrumental intensity*
1	MYG004	2933gal	6.6
2	MYG012	2019gal	6.0
3	IBR003	1845gal	6.4
4	MYG013	1808gal	6.3
5	IBR013	1762gal	6.4
6	FKSH10	1335gal	6.0
7	TCGH16	1305gal	6.5
8	TCG014	1291gal	6.3
9	IBRH11	1224gal	6.2
10	MYGH10	1137gal	6.0
*JMA: Japan Meteorological Agency			
(MYG: Miyagi Prefecture, IBR: Ibaragi Prefecture, FKS: Fukushima Prefecture, TCG: Tochigi Prefecture. This list is based on information obtained by March 13, 2011 from 276 K-NET and 112 KiK-net sites.)			

Table 2 Cross sections of members

Story	Column (mm)	Beam (mm)
31 - 40	600×600×20×20	850×300×15×25
21 - 30	800×800×25×25	850×300×15×25
11 - 20	1000×1000×35×35	850×300×20×30
1 - 10	1000×1000×45×45	1000×300×20×40

Table 3 Reduction of top acceleration via high-hardness rubber dampers (m/s^2)

60-story building	EW component of TKY007	EW component at Chiyoda-ku station	NS component at Osaka WTC
No damper	1.79	1.54	0.933
With damper	1.65	1.21	0.667

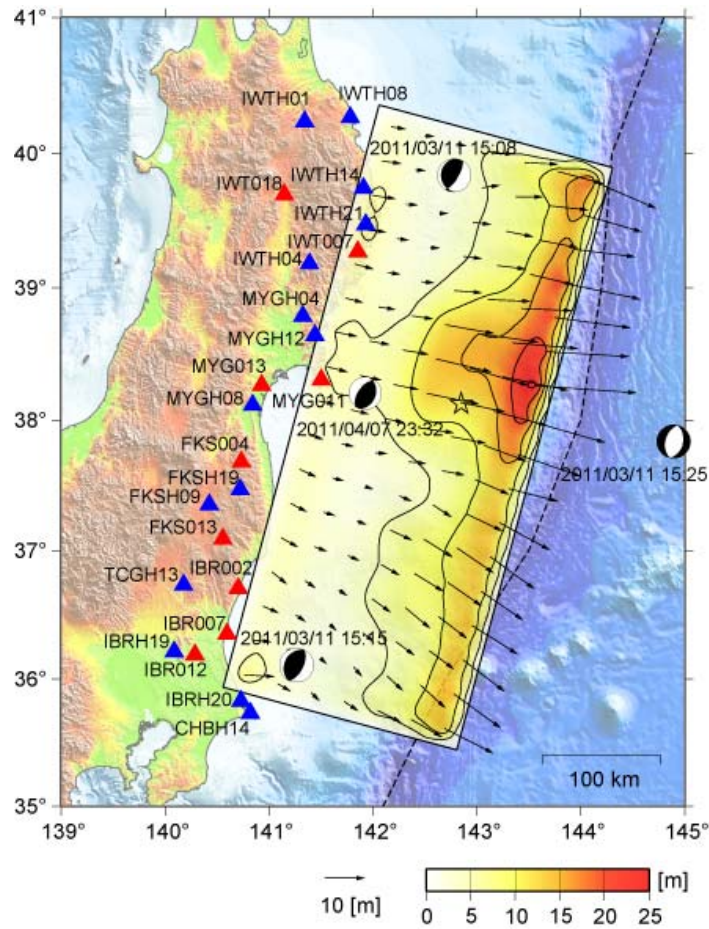


Fig.1 Source inversion and slip distribution using near-source strong ground motions [15]

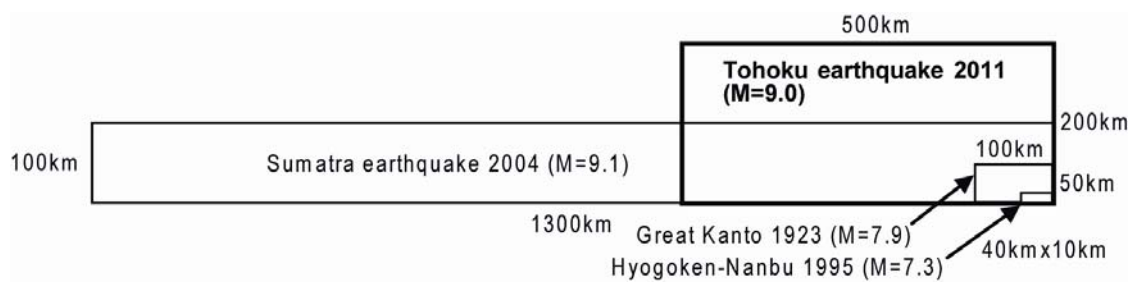


Fig.2 Fault size of 2004 Sumatra earthquake (M=9.1), 1923 Great Kanto earthquake (M=7.9), 1995 Hyogoken-Nanbu (Kobe) earthquake (M=7.3) and 2011 off the Pacific coast of Tohoku earthquake (M=9.0) (data from [16])

Characteristics of near-source ground motions

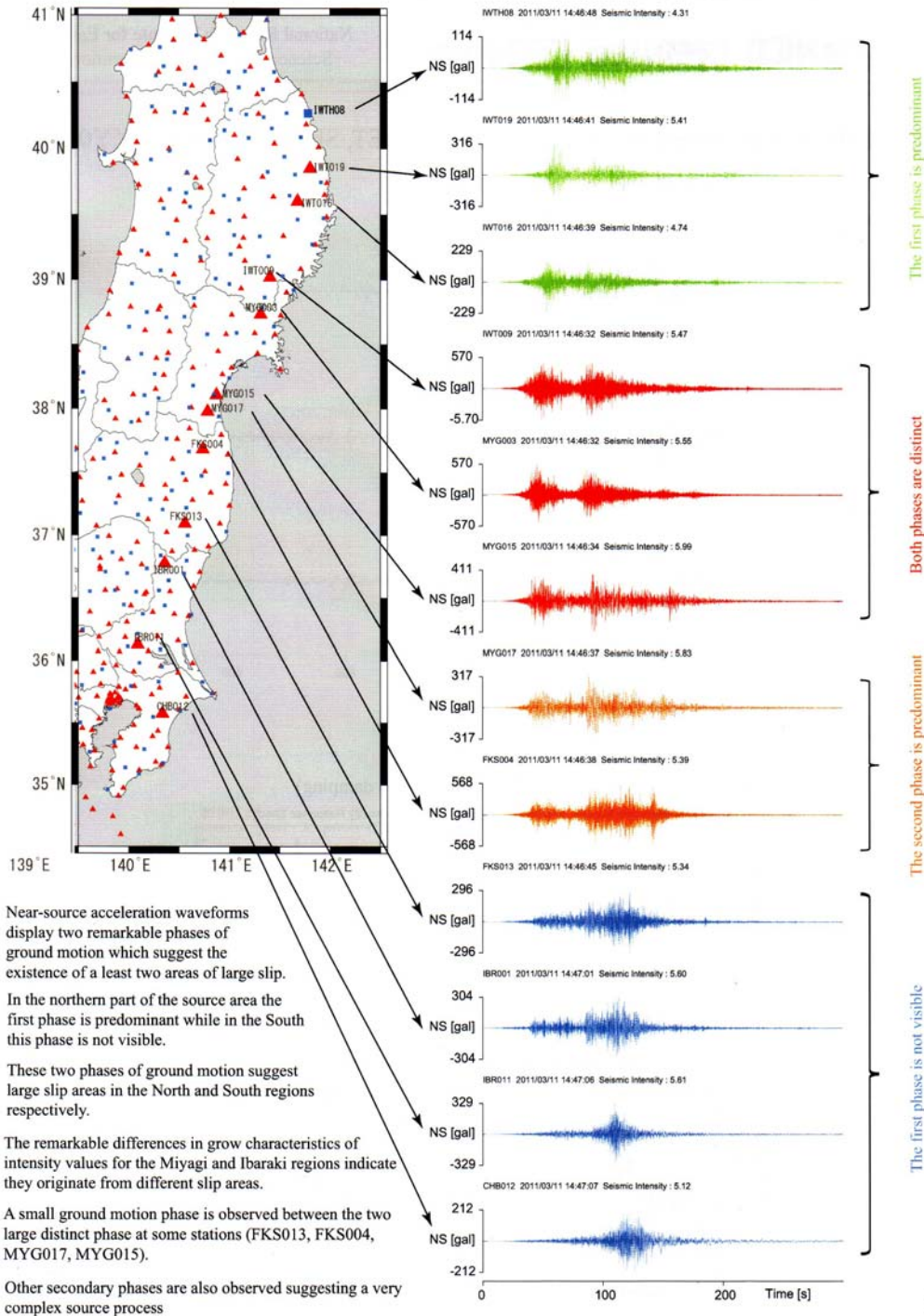


Fig.3(a) Characteristics of near-source ground motions along Pacific coast in East Japan [17]

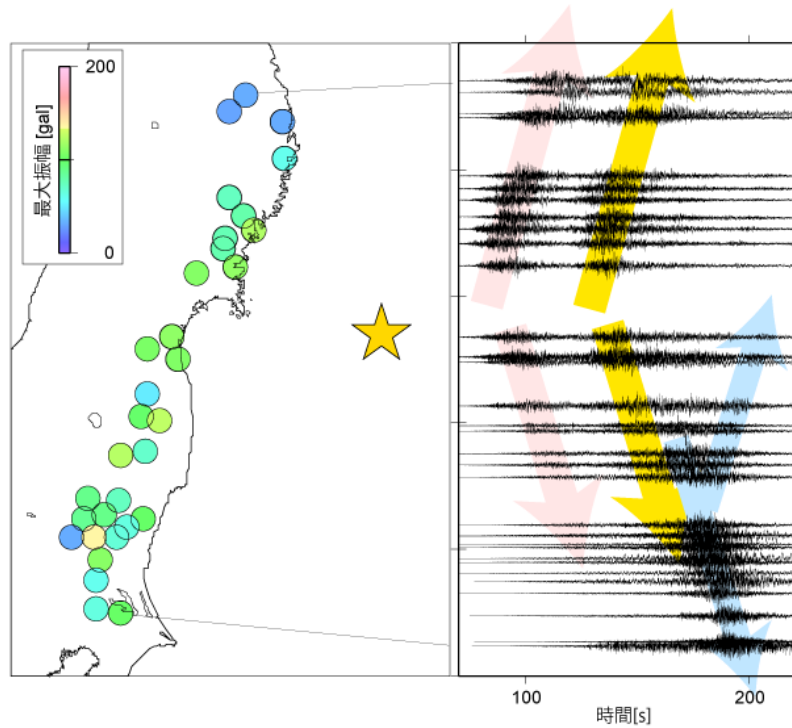


Fig.3(b) Relation among fault rupture, wave propagation and ground motion sequences (Yellow star indicates the epicenter) [21]

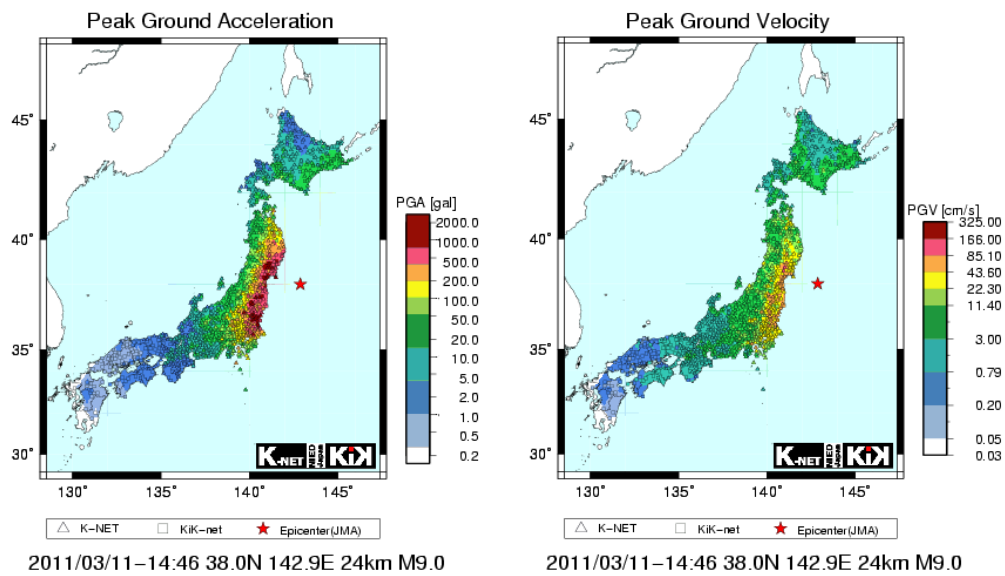


Fig.4 Maximum ground accelerations and maximum ground velocities determined from K-NET and KiK-net data [22]

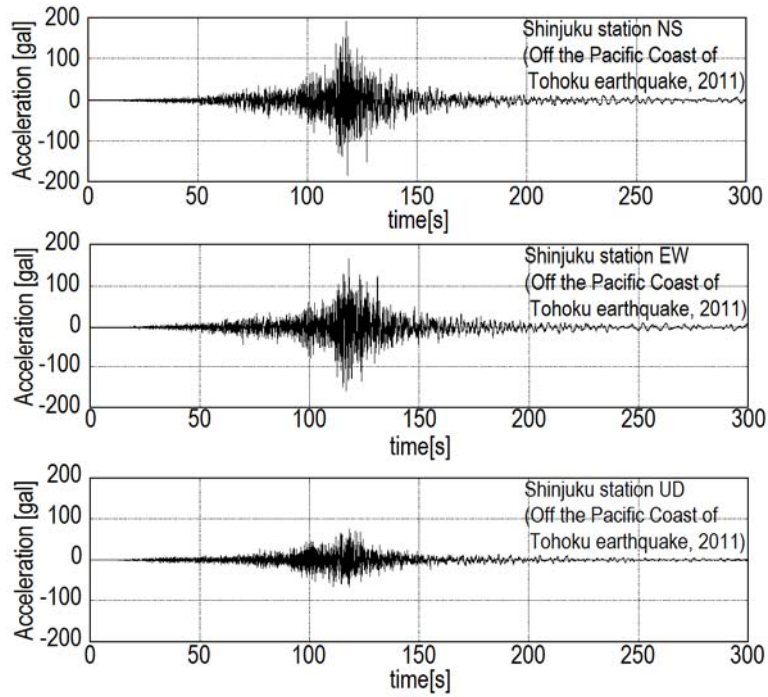


Fig.5(a) Long-period acceleration ground motion recorded at K-NET, Shinjuku station (TKY007)

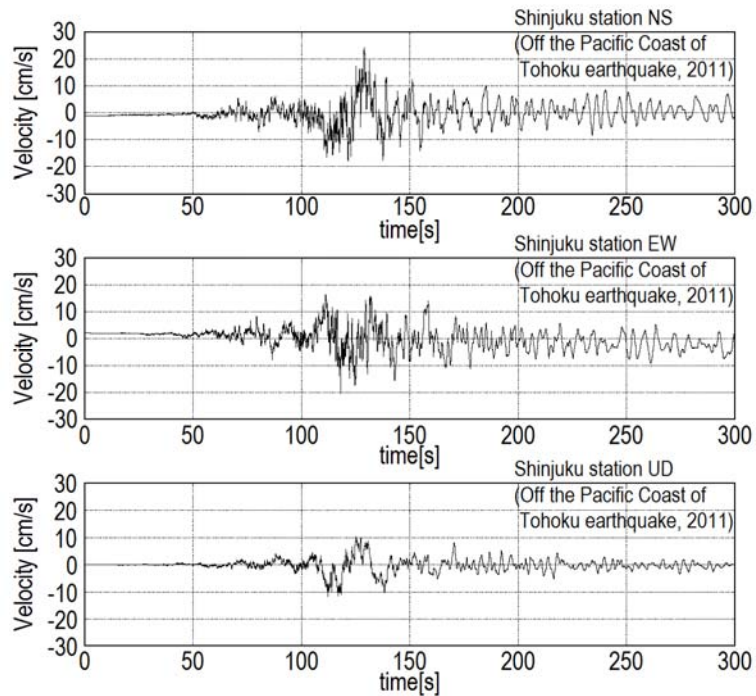


Fig.5(b) Long-period velocity ground motion recorded at K-NET, Shinjuku station (TKY007)

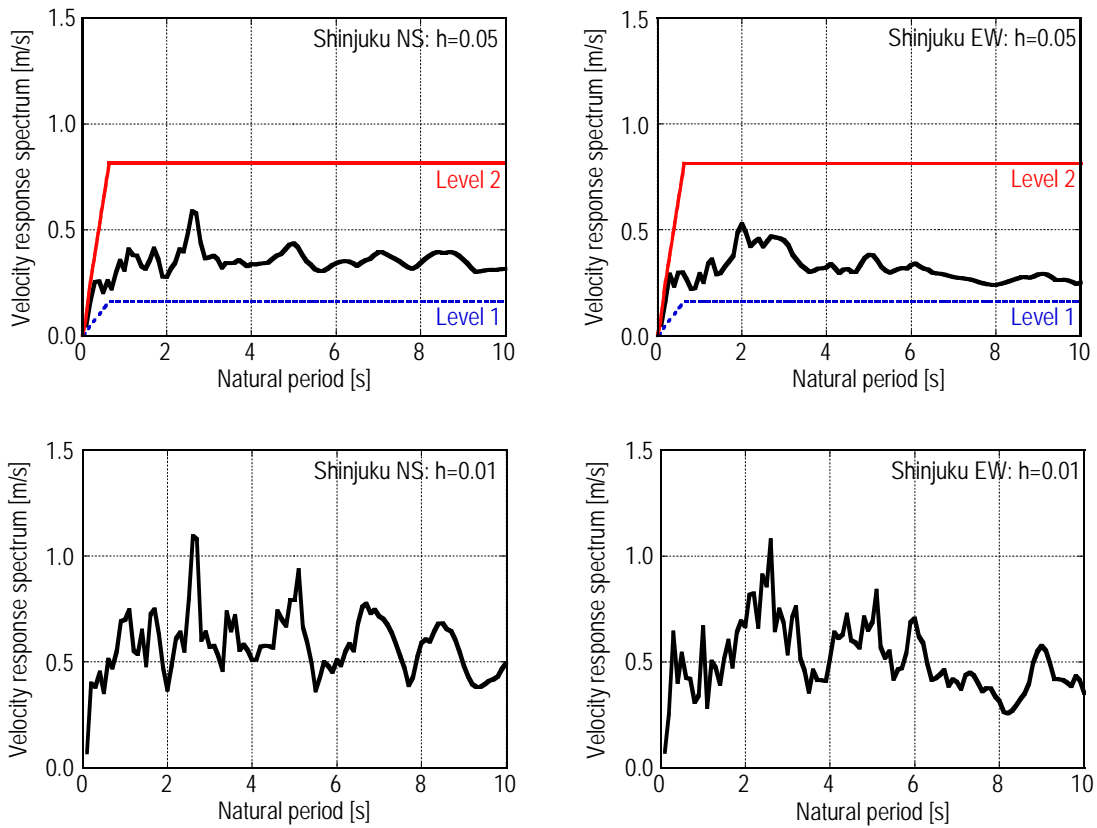


Fig.6 Velocity response spectra (5% and 1% damping) of ground motions at Shinjuku station (TKY007) and the corresponding ones of Japanese seismic design code for 5% damping

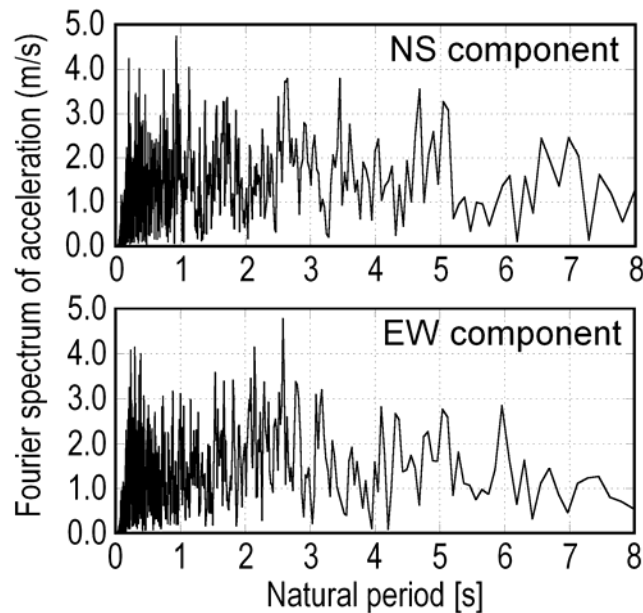


Fig.7 Fourier amplitude spectra of acceleration ground motion at K-NET, Shinjuku station (TKY007)

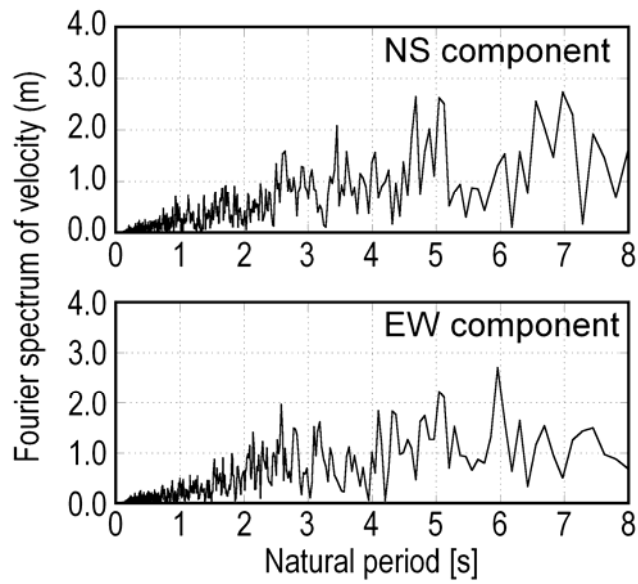


Fig.8 Fourier amplitude spectra of velocity ground motion at K-NET, Shinjuku station (TKY007)

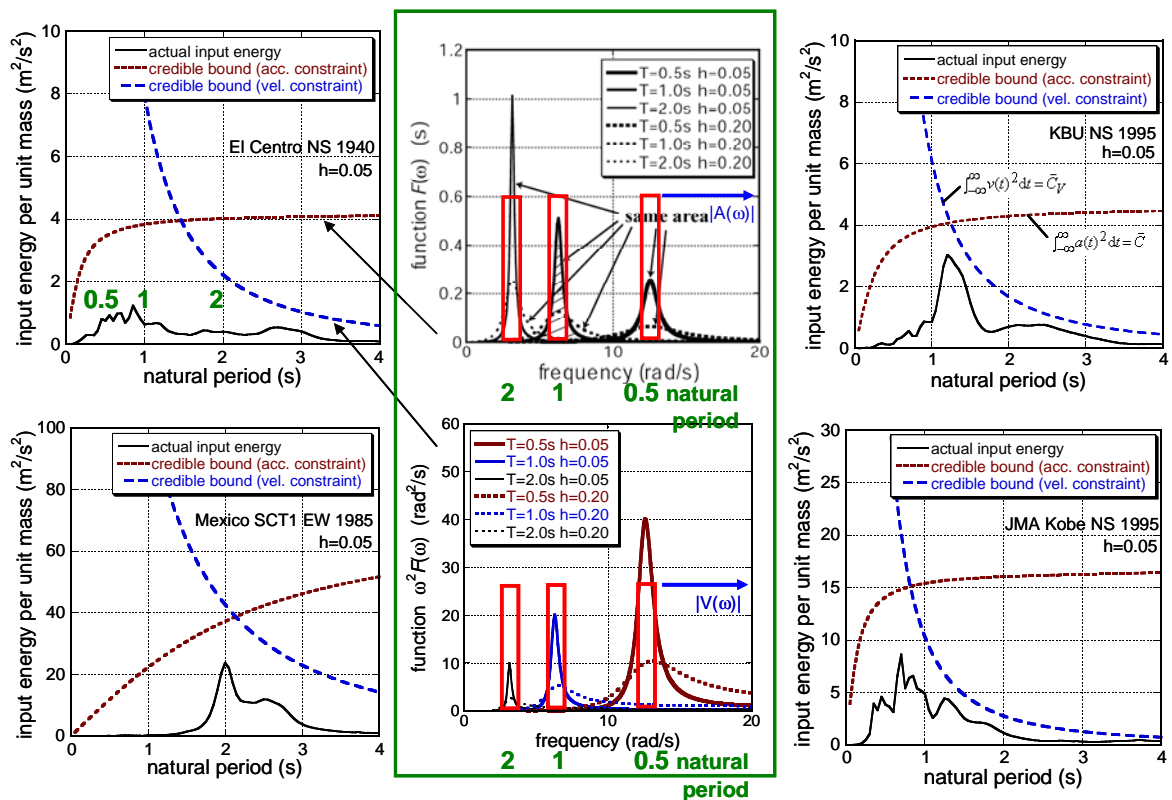


Fig.9 Schematic diagram for computing credible bounds for acceleration and velocity constraints

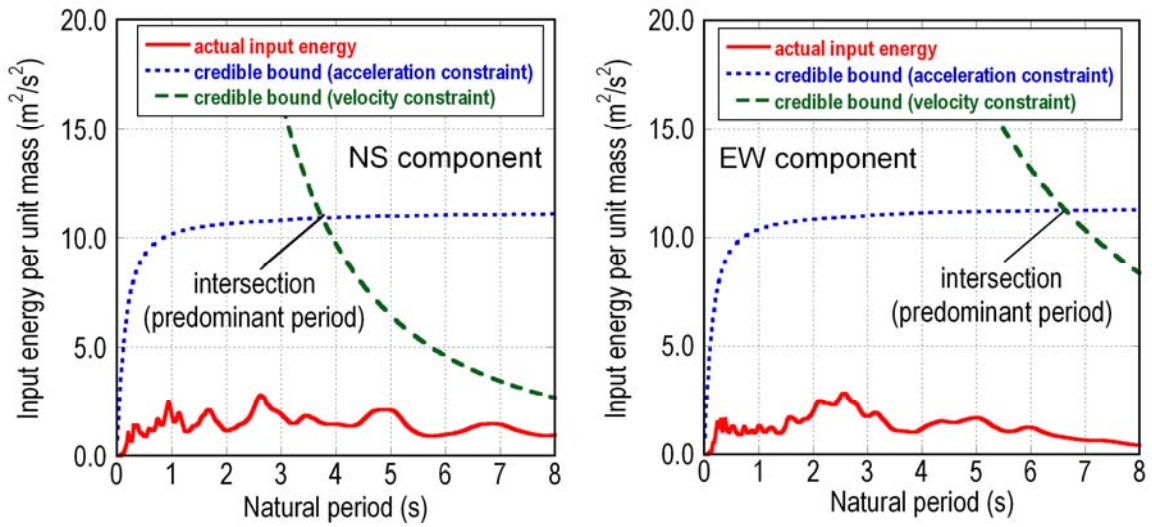


Fig.10(a) Actual input energies per unit mass (5% damping), the credible bounds for acceleration constraints and the credible bounds for velocity constraints for the ground motions at K-NET, Shinjuku station (TKY007)

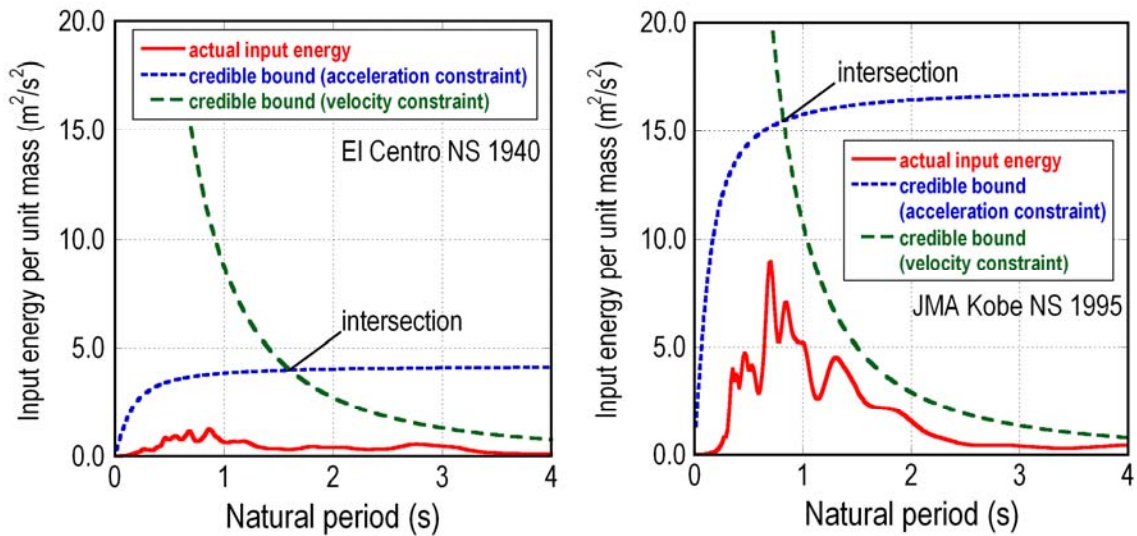


Fig.10(b) Actual input energies per unit mass (5% damping), the credible bounds for acceleration constraints and the credible bounds for velocity constraints for El Centro NS (1940) and JMA Kobe NS (1995)

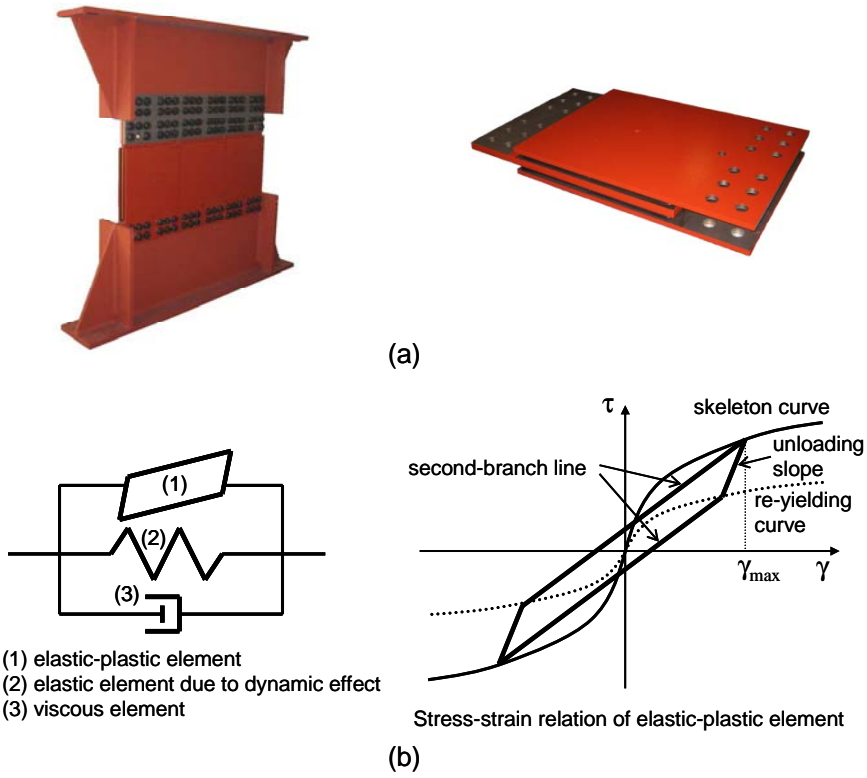


Fig.11 High-hardness rubber dampers; (a) Overview, (b) Modeling into three elements

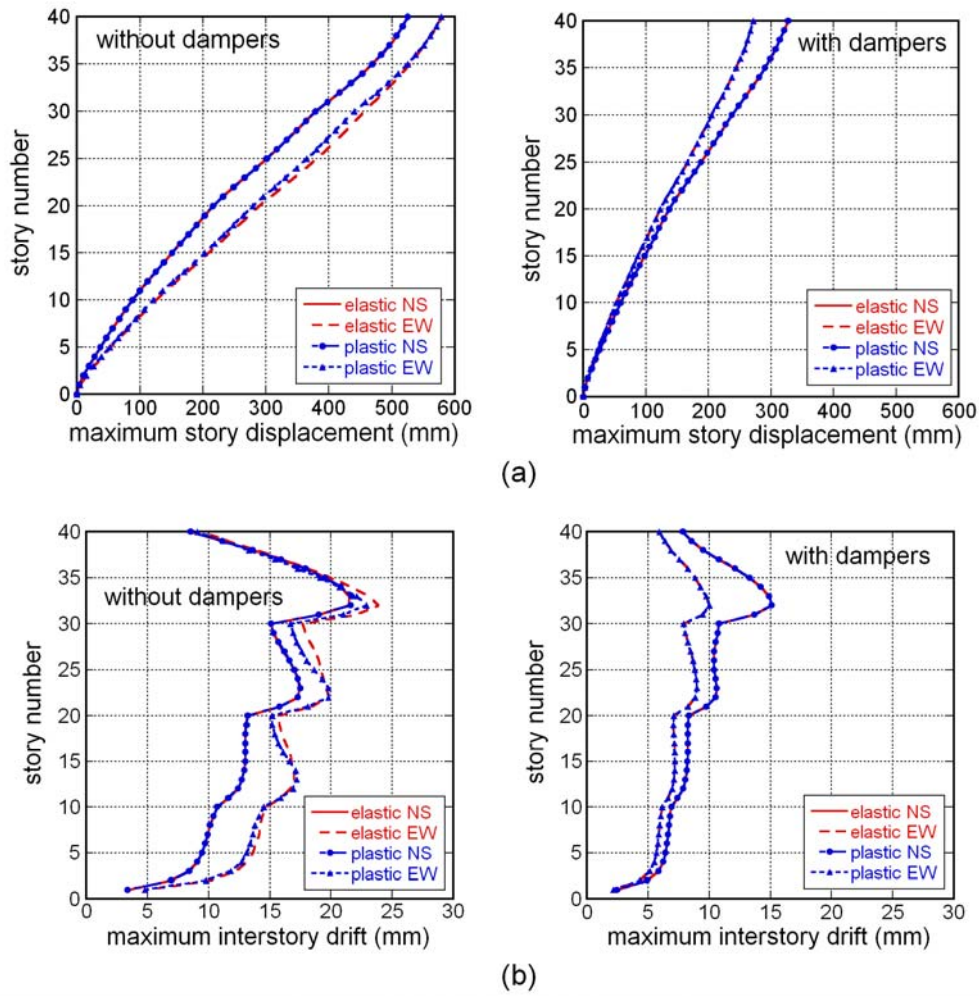


Fig.12 (a) Maximum story displacement and (b) maximum interstory drift of a 40-story building of $T_1=4.14s$ without or with high-hardness rubber dampers to ground motion at Shinjuku station (TKY007) during the 2011 off the Pacific coast of Tohoku earthquake (frame response: elastic or elastic-plastic)

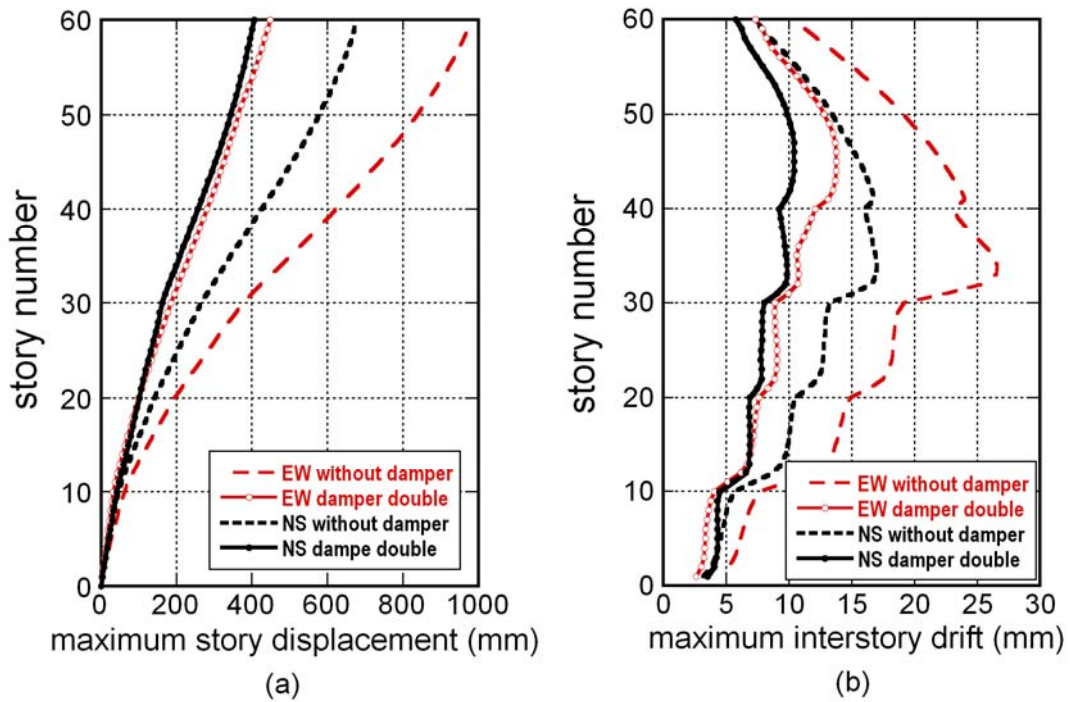


Fig.13 (a) Maximum story displacement and (b) maximum interstory drift of a 60-story building of $T_1=5.92s$ without or with high-hardness rubber dampers to ground motion at Shinjuku station (TKY007) during the 2011 off the Pacific coast of Tohoku earthquake (frame response: elastic-plastic, '4 dampers per story' corresponds to 'damper double')

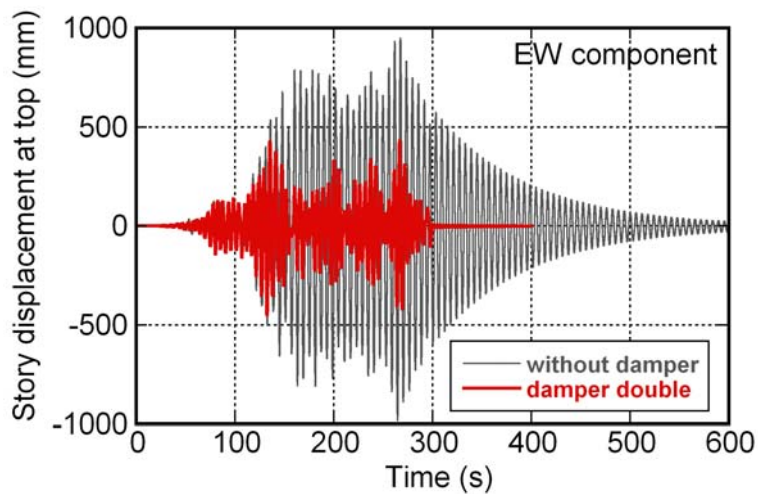


Fig.14(a) Comparison of time histories of top-story displacement of an assumed 60-story building of $T_1=5.92s$ without or with high-hardness rubber dampers to ground motion at Shinjuku station (EW component of TKY007) during the 2011 off the Pacific coast of Tohoku earthquake (frame response: elastic-plastic)

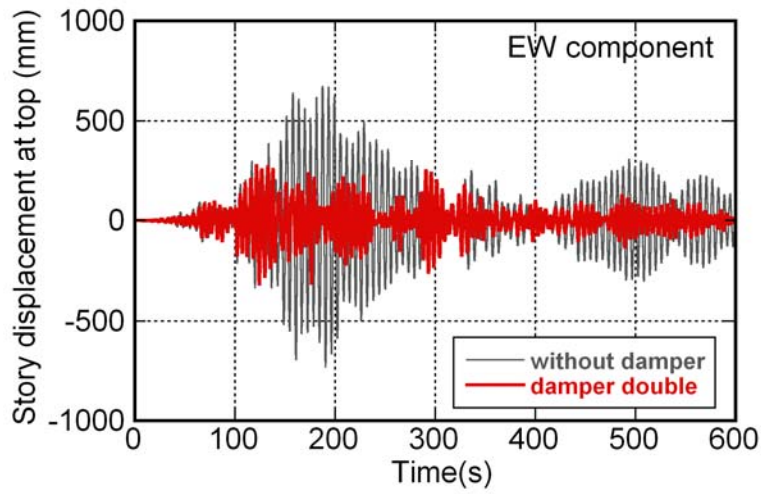


Fig.14(b) Comparison of time histories of top-story displacement of an assumed 60-story building of $T_1=5.92s$ without or with high-hardness rubber dampers to ground motion (EW component) at Chiyoda-ku station near Shinjuku station during the 2011 off the Pacific coast of Tohoku earthquake (frame response: elastic-plastic)

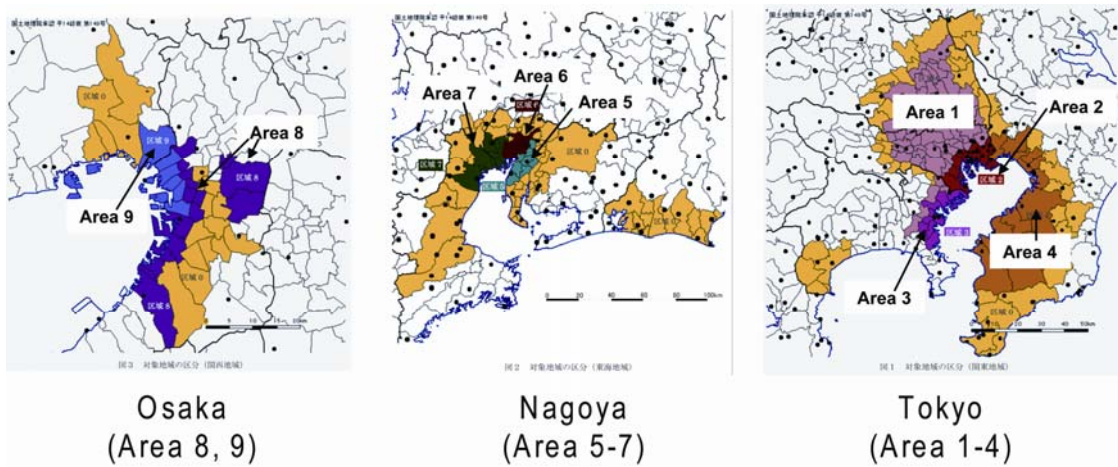


Fig.15 Nine areas in Osaka, Nagoya and Tokyo specified by the MLIT of Japan [5]

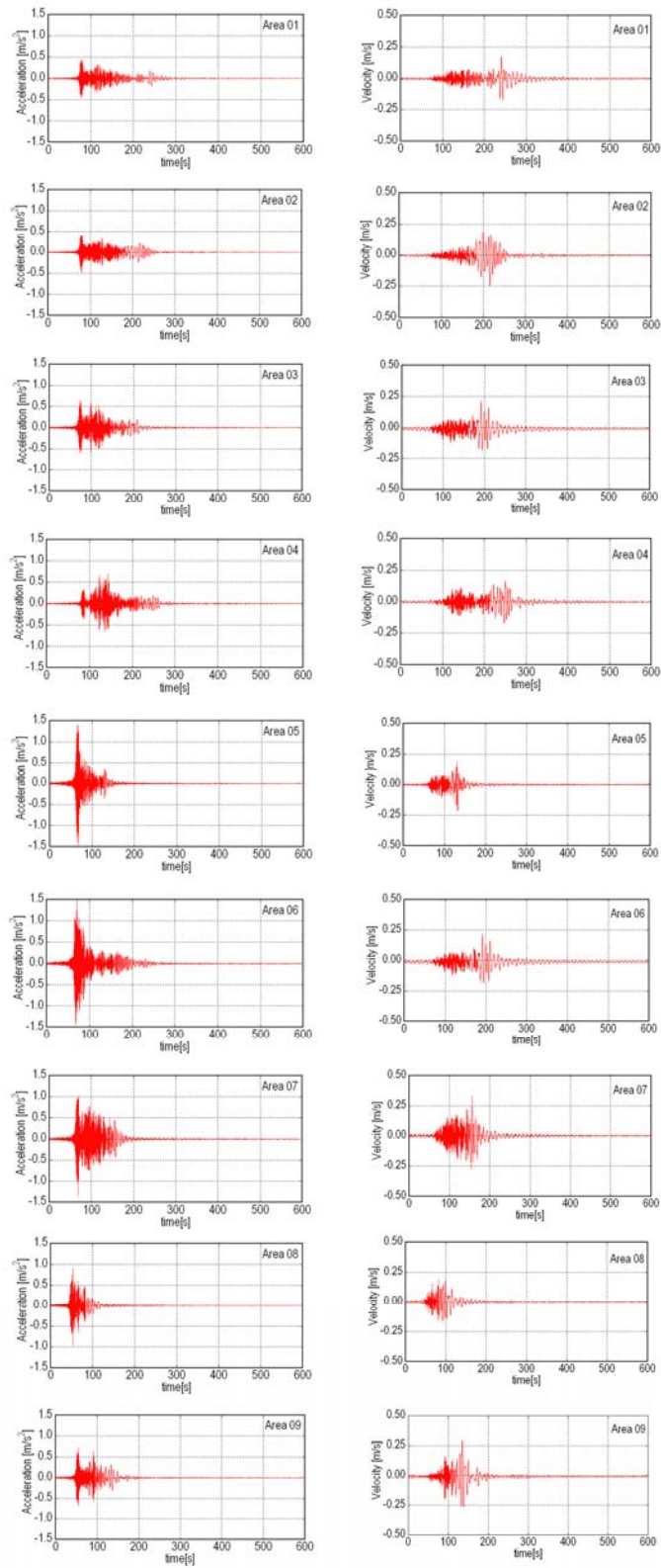


Fig.16 Acceleration and velocity ground motion records at 9 areas specified by the MLIT of Japan (data from [5])

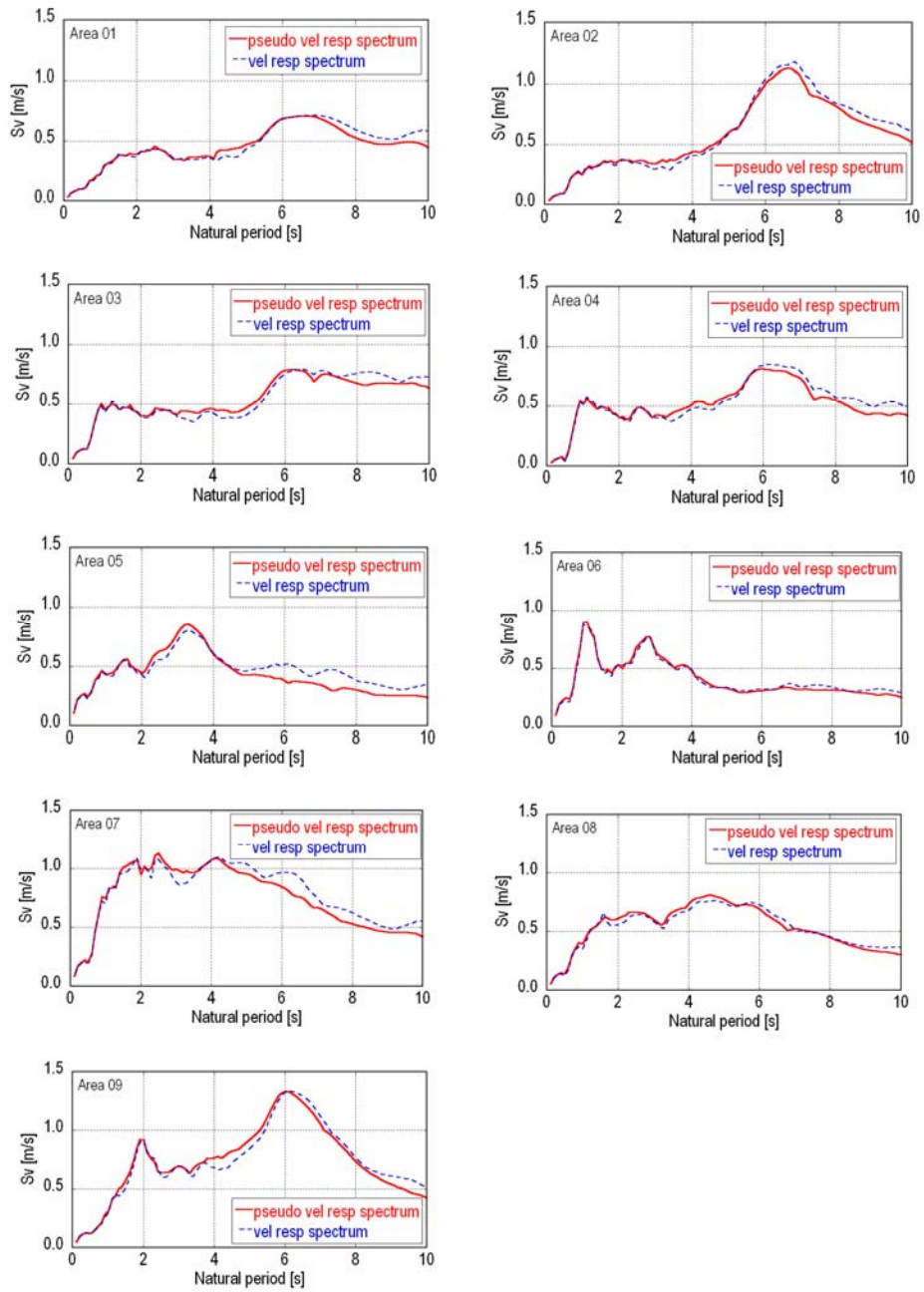


Fig.17 Pseudo velocity response spectra (5% damping) and velocity response spectra of the simulated acceleration ground motions specified by the MLIT of Japan [5]

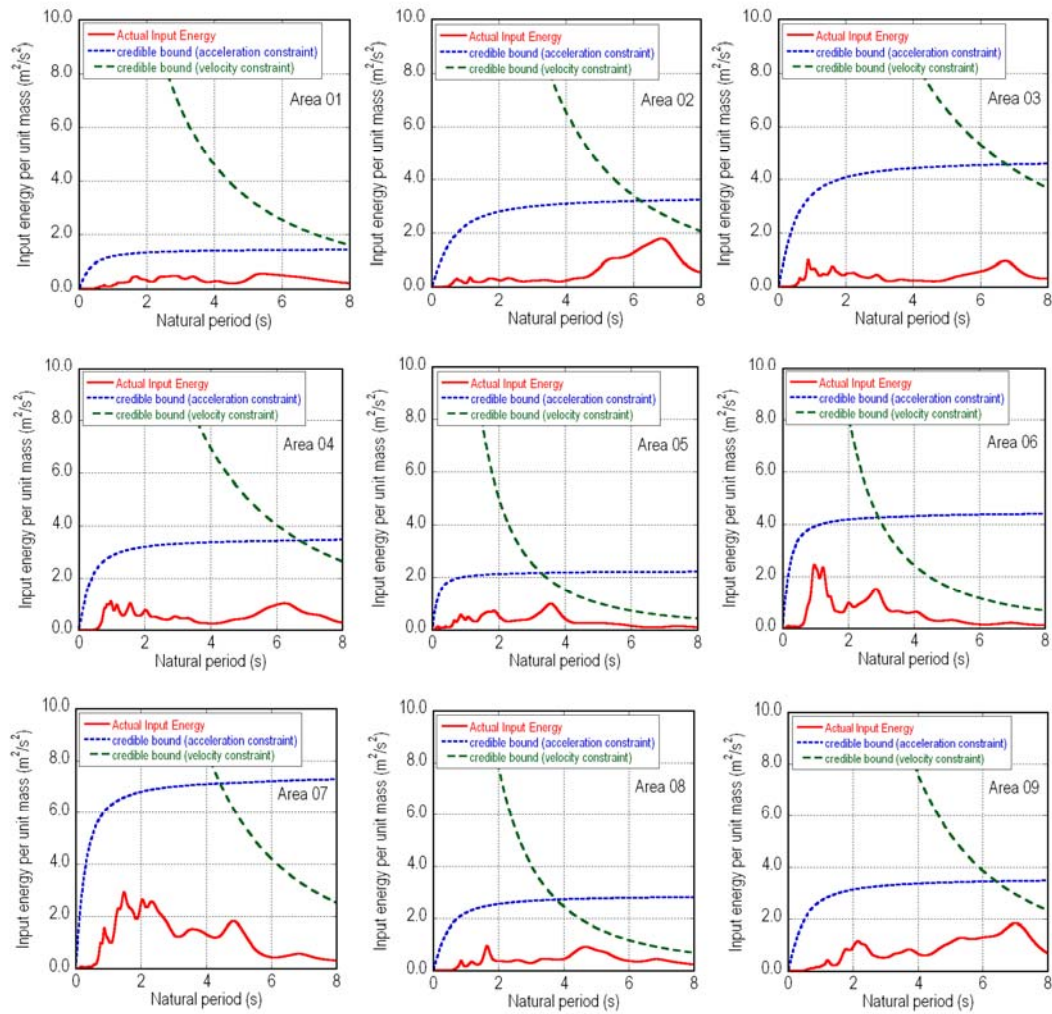


Fig.18 Actual input energies per unit mass (5% damping), the credible bounds for acceleration constraints and the credible bounds for velocity constraints for the simulated ground motions specified by the MLIT of Japan

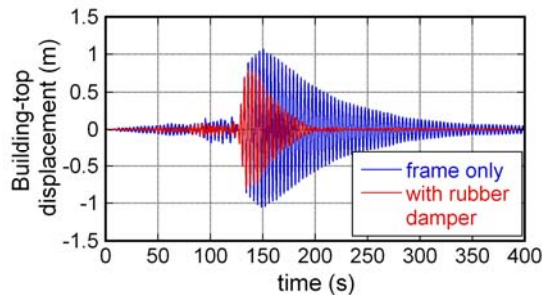


Fig.19 Comparison of the time histories of the top displacement of the 40-story buildings of $T_1=3.6s$ without and with high-hardness rubber dampers (frame response; elastic) under a simulated long-period ground motion in area 5

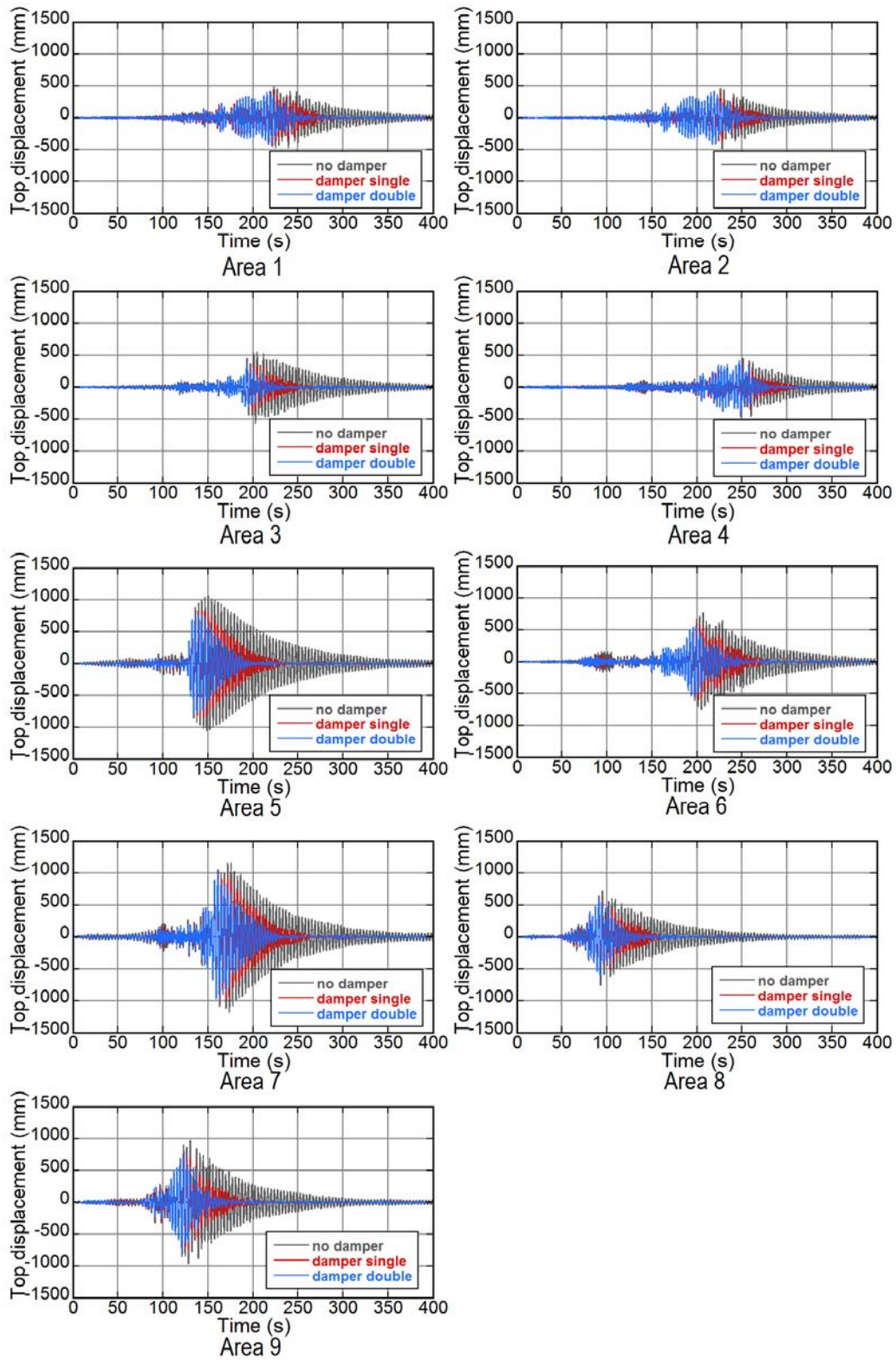


Fig.20 Time histories of top displacement of 40-story buildings of $T_1=3.6s$ without and with high-hardness rubber dampers (frame response; elastic)

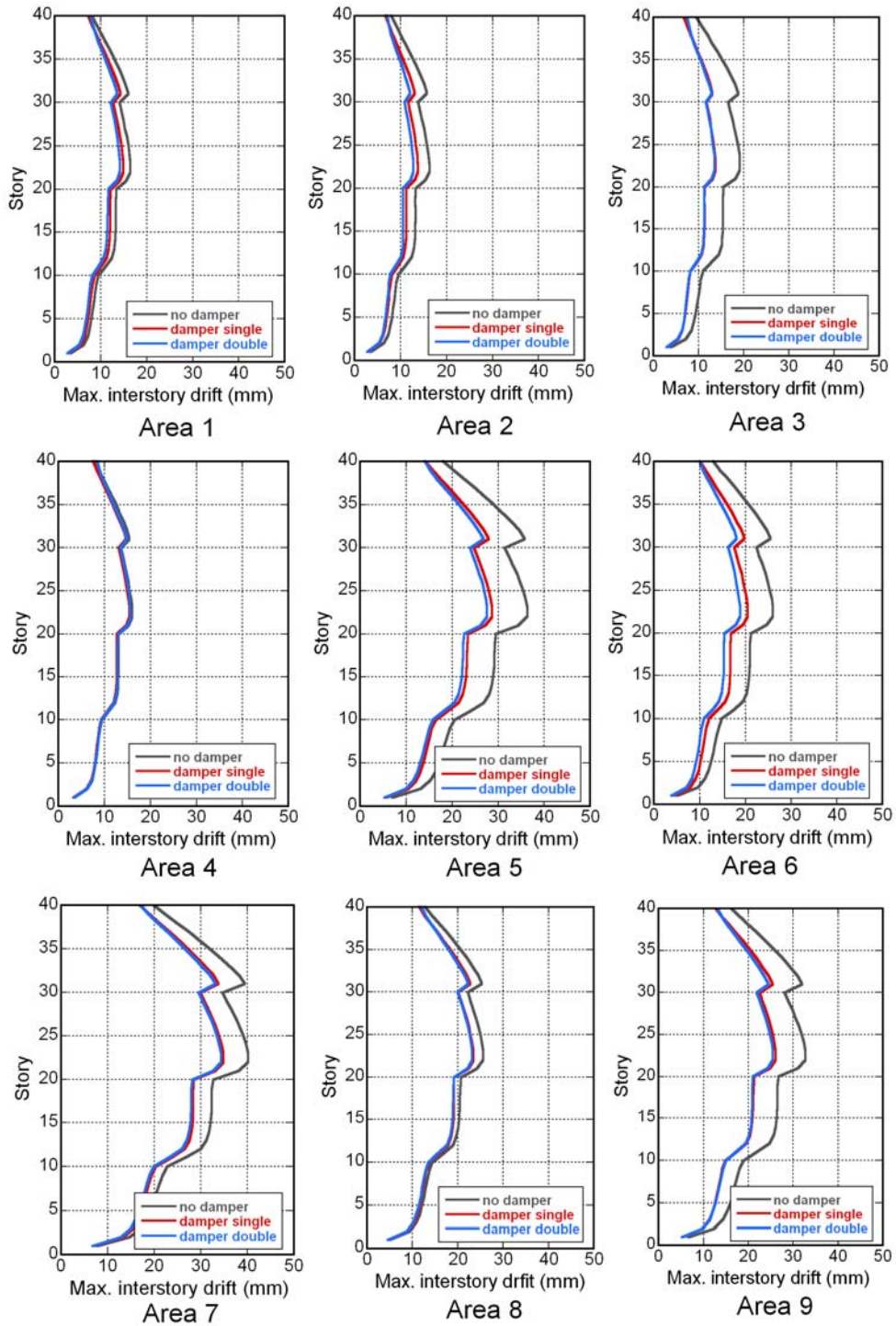


Fig.21 Maximum interstory drifts of 40-story buildings of $T_1=3.6s$ without and with high-hardness rubber dampers (frame response; elastic)

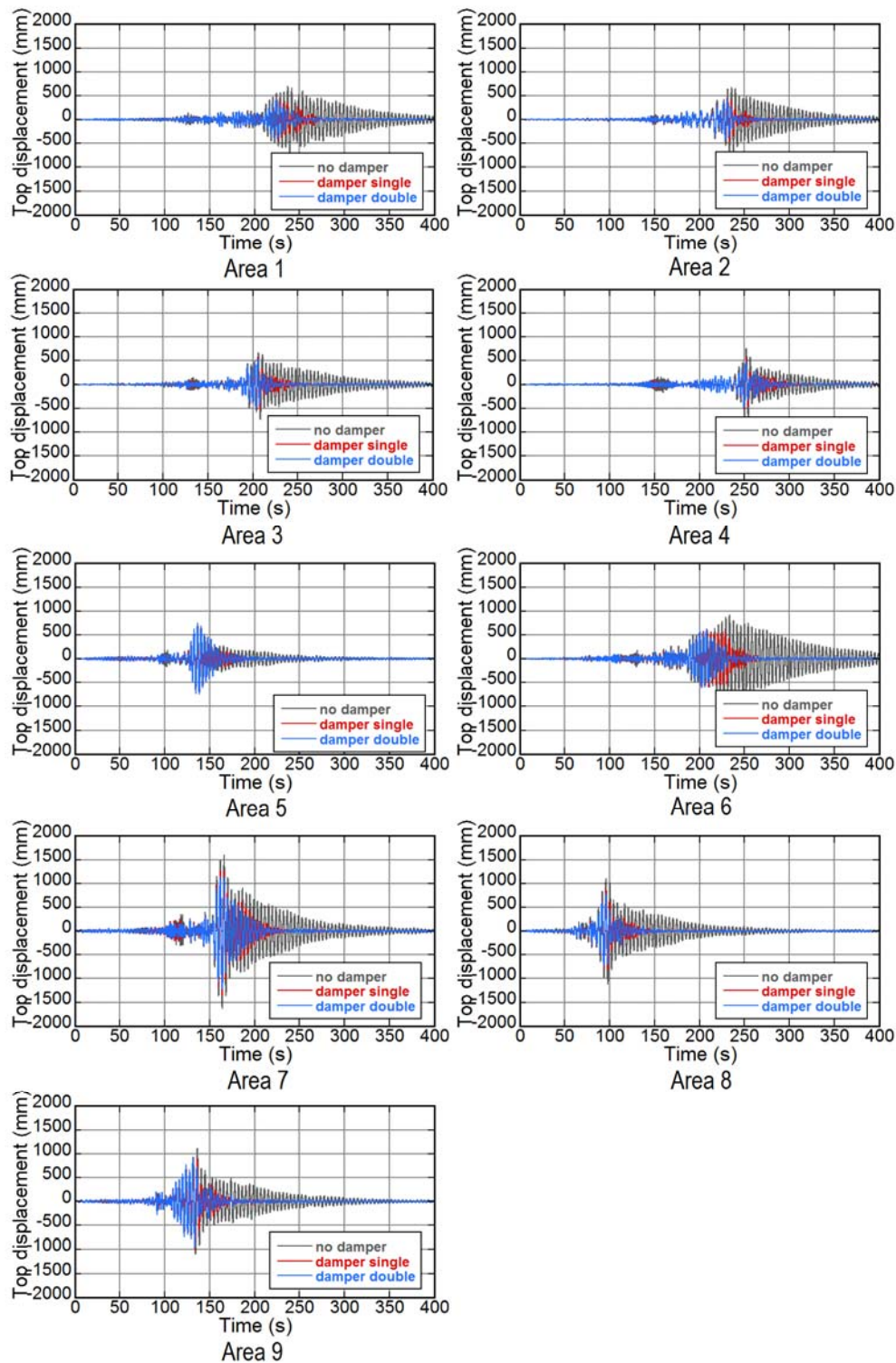


Fig.22 Time histories of top displacement of 40-story buildings of $T_1=4.14s$ without and with high-hardness rubber dampers (frame response; elastic)

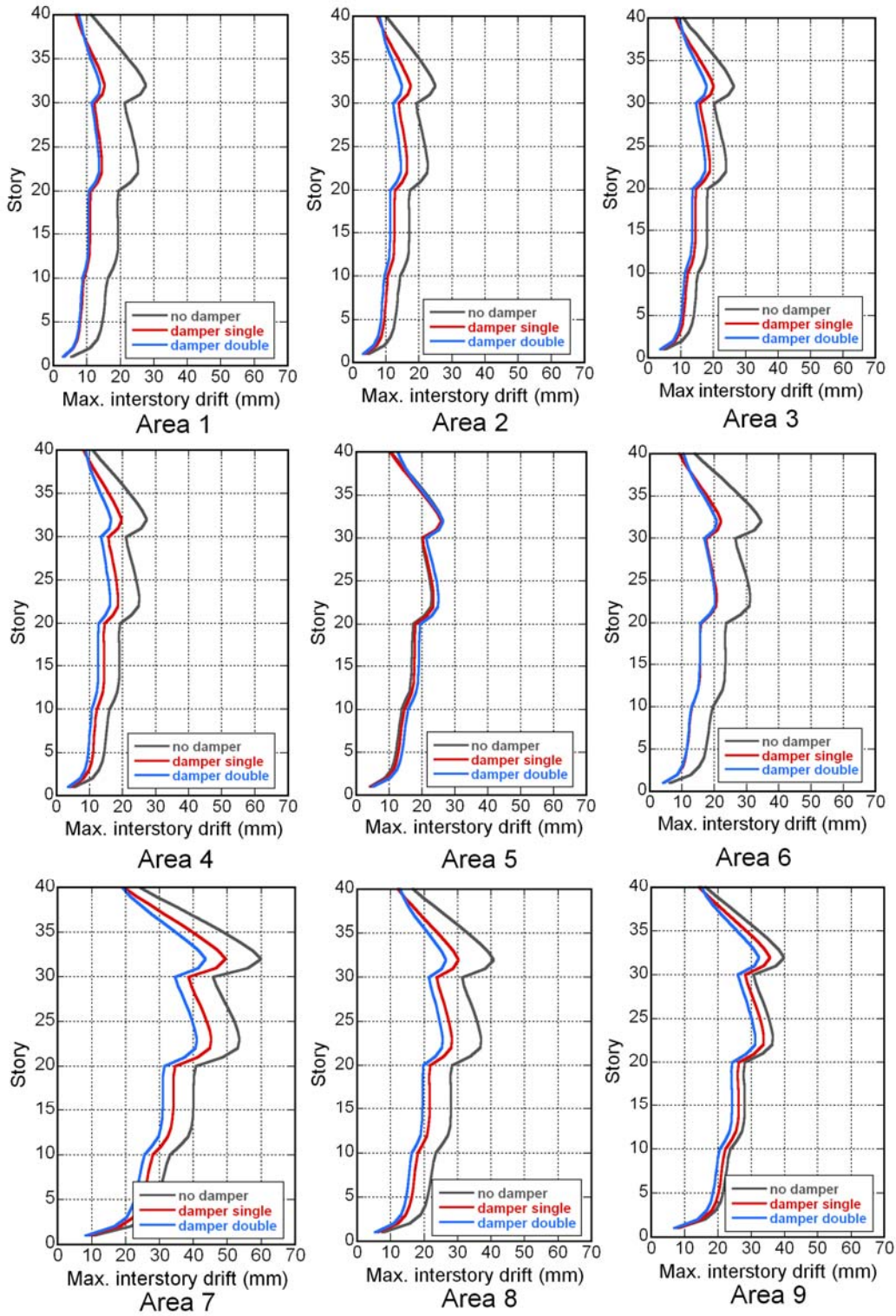


Fig.23 Maximum interstory drifts of 40-story buildings of $T_1=4.14s$ without and with high-hardness rubber dampers (frame response; elastic)

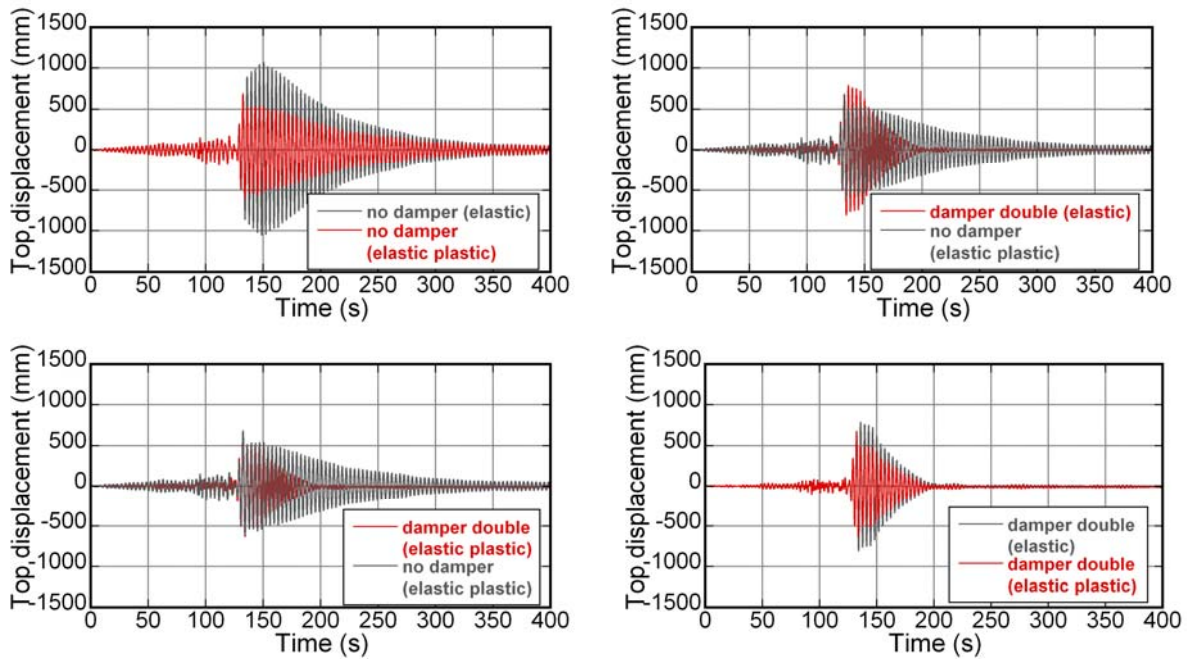


Fig.24 Top displacement of 40-story buildings of $T_1=3.6(s)$ without and with high-hardness rubber dampers (frame response: elastic or elastic-plastic) (Area 5)

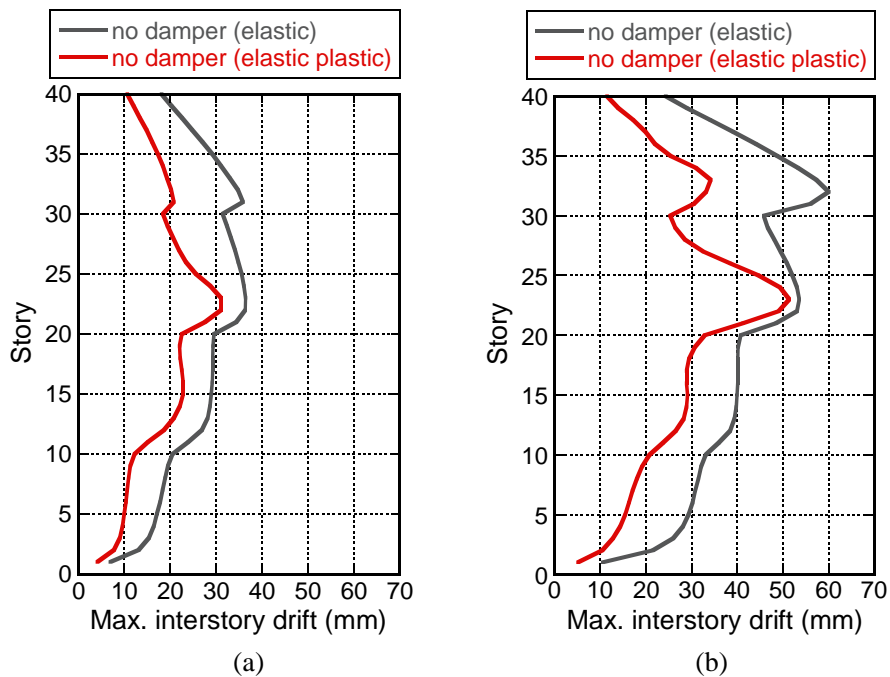


Fig.25 Maximum interstory drifts of 40-story buildings of $T_1=3.6s$ and $T_1=4.14s$ without high-hardness rubber dampers (frame response; elastic or elastic-plastic), (a) 40-story building of $T_1=3.6s$ in Area 5, (b) 40-story building of $T_1=4.14s$ in Area 7

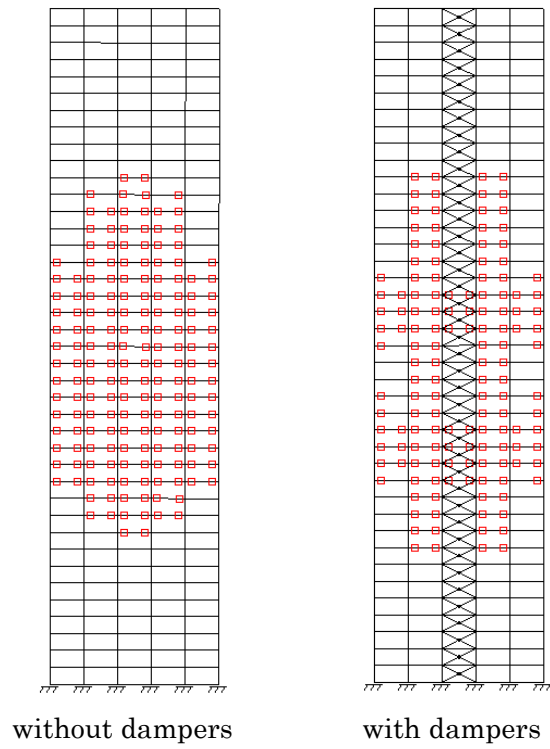


Fig.26 Plastic-hinge formation in 40-story buildings of $T_1=3.6(s)$ without and with high-hardness rubber dampers (Area 5)